



Evidence for light-by-light scattering and searches for axion-like particles in ultraperipheral PbPb collisions at $\sqrt{s_{NN}} = 5.02$ TeV

The CMS Collaboration^{*}

CERN, Switzerland

ARTICLE INFO

Article history:

Received 10 October 2018
 Received in revised form 18 July 2019
 Accepted 29 July 2019
 Available online 1 August 2019
 Editor: M. Doser

Keywords:

Light-by-light
 CMS
 UPC
 Photoproduction
 PbPb

ABSTRACT

Evidence for the light-by-light scattering process, $\gamma\gamma \rightarrow \gamma\gamma$, in ultraperipheral PbPb collisions at a centre-of-mass energy per nucleon pair of 5.02 TeV is reported. The analysis is conducted using a data sample corresponding to an integrated luminosity of $390 \mu\text{b}^{-1}$ recorded by the CMS experiment at the LHC. Light-by-light scattering processes are selected in events with two photons exclusively produced, each with transverse energy $E_T^\gamma > 2$ GeV, pseudorapidity $|\eta^\gamma| < 2.4$, diphoton invariant mass $m^{\gamma\gamma} > 5$ GeV, diphoton transverse momentum $p_T^{\gamma\gamma} < 1$ GeV, and diphoton acoplanarity below 0.01. After all selection criteria are applied, 14 events are observed, compared to expectations of 9.0 ± 0.9 (theo) events for the signal and 4.0 ± 1.2 (stat) for the background processes. The excess observed in data relative to the background-only expectation corresponds to a significance of 3.7 standard deviations, and has properties consistent with those expected for the light-by-light scattering signal. The measured fiducial light-by-light scattering cross section, $\sigma_{\text{fid}}(\gamma\gamma \rightarrow \gamma\gamma) = 120 \pm 46$ (stat) ± 28 (syst) ± 12 (theo) nb, is consistent with the standard model prediction. The $m^{\gamma\gamma}$ distribution is used to set new exclusion limits on the production of pseudoscalar axion-like particles, via the $\gamma\gamma \rightarrow a \rightarrow \gamma\gamma$ process, in the mass range $m_a = 5\text{--}90$ GeV.

© 2019 The Author(s). Published by Elsevier B.V. This is an open access article under the CC BY license (<http://creativecommons.org/licenses/by/4.0/>). Funded by SCOAP³.

1. Introduction

Elastic light-by-light (LbL) scattering, $\gamma\gamma \rightarrow \gamma\gamma$, is a pure quantum mechanical process that proceeds, at leading order in the quantum electrodynamics (QED) coupling α , via virtual box diagrams containing charged particles (Fig. 1, left). In the standard model (SM), the box diagram involves contributions from charged fermions (leptons and quarks) and the W^\pm boson. Although LbL scattering via an electron loop has been indirectly tested through the high-precision measurements of the anomalous magnetic moment of the electron [1] and muon [2], its direct observation in the laboratory remains elusive because of a very suppressed production cross section proportional to $\alpha^4 \approx 3 \times 10^{-9}$. Out of the two closely-related processes—photon scattering in the Coulomb field of a nucleus (Delbrück scattering) [3] and photon splitting in a strong magnetic field (“vacuum birefringence”) [4,5]—only the former has been clearly observed [6]. However, as demonstrated in Ref. [7], the LbL process can be experimentally observed in ultraperipheral interactions of ions, with impact parameters larger than twice the radius of the nuclei, exploiting the very large

fluxes of quasireal photons emitted by the nuclei accelerated at TeV energies [8]. Ions accelerated at high energies generate strong electromagnetic fields, which, in the equivalent photon approximation [9–11], can be considered as γ beams of virtuality $Q^2 < 1/R^2$, where R is the effective radius of the charge distribution. For lead (Pb) nuclei with radius $R \approx 7$ fm, the quasireal photon beams have virtualities $Q^2 < 10^{-3} \text{ GeV}^2$, but very large longitudinal energy (up to $E_\gamma = \gamma/R \approx 80$ GeV, where γ is the Lorentz relativistic factor), enabling the production of massive central systems with very soft transverse momenta ($p_T \lesssim 0.1$ GeV). Since each photon flux scales as the square of the ion charge Z^2 , $\gamma\gamma$ scattering cross sections in PbPb collisions are enhanced by a factor of $Z^4 \simeq 5 \times 10^7$ compared to similar proton-proton or electron-positron interactions.

Many final states have been measured in photon-photon interactions in ultraperipheral collisions of proton and/or lead beams at the CERN LHC, including $\gamma\gamma \rightarrow e^+e^-$ [12–21], $\gamma\gamma \rightarrow W^+W^-$ [22–24], and first evidence of $\gamma\gamma \rightarrow \gamma\gamma$ reported by the ATLAS experiment [25] with a signal significance of 4.4 standard deviations (3.8 standard deviations expected). The final-state signature of interest in this analysis is the exclusive production of two photons, $\text{PbPb} \rightarrow \gamma\gamma \rightarrow \text{Pb}^{(*)}\gamma\gamma\text{Pb}^{(*)}$, where the diphoton final state is measured in the otherwise empty central part of the detector, and the outgoing Pb ions (with a potential electromagnetic ex-

^{*} E-mail address: cms-publication-committee-chair@cern.ch.

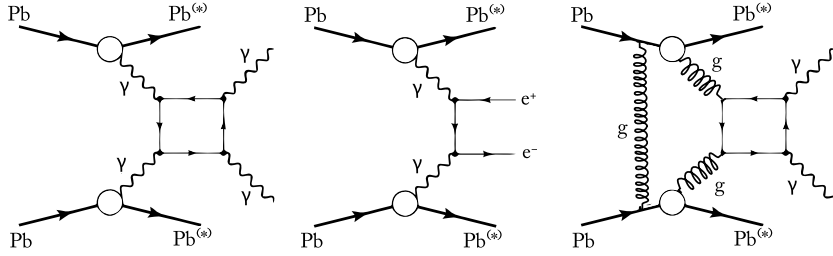


Fig. 1. Schematic diagrams of light-by-light scattering ($\gamma\gamma \rightarrow \gamma\gamma$, left), QED dielectron ($\gamma\gamma \rightarrow e^+e^-$, centre), and central exclusive diphoton ($gg \rightarrow \gamma\gamma$, right) production in ultraperipheral PbPb collisions. The $(^*)$ superscript indicates a potential electromagnetic excitation of the outgoing ions.

citation denoted by the $(^*)$ superscript) survive the interaction and escape undetected at very low θ angles with respect to the beam direction (Fig. 1, left). The dominant backgrounds are the QED production of an exclusive electron-positron pair ($\gamma\gamma \rightarrow e^+e^-$) where the e^\pm are misidentified as photons (Fig. 1, centre), and gluon-induced central exclusive production (CEP) [26] of a pair of photons (Fig. 1, right).

The $\gamma\gamma \rightarrow \gamma\gamma$ process at the LHC has been proposed as a particularly sensitive channel to study physics beyond the SM. Modifications of the LbL scattering rates can occur if, e.g. new heavy particles, such as magnetic monopoles [27], vector-like fermions [28], or dark sector particles [29], contribute to the virtual corrections of the box depicted in Fig. 1. Other new spin-even particles, such as axion-like particles (ALPs) [30] or gravitons [31], can also contribute to the LbL scattering continuum or to new diphoton resonances. In addition, light-by-light cross sections are sensitive to Born-Infeld extensions of QED [32], and anomalous quartic gauge couplings [33].

We report a study of the $\gamma\gamma \rightarrow \gamma\gamma$ process, using PbPb collision data recorded by the CMS experiment in 2015 at $\sqrt{s_{NN}} = 5.02$ TeV and corresponding to an integrated luminosity of $390 \mu\text{b}^{-1}$. A comparison of exclusive diphoton and dielectron yields, with almost identical event selection and reconstruction efficiencies, is provided as a function of key kinematic variables to check of the robustness of the analysis. The ratio of the LbL scattering to QED e^+e^- production cross sections is reported, so as to reduce the dependence on various experimental corrections and uncertainties. Using the measured $m^{\gamma\gamma}$ distribution, new exclusion limits are set on ALP production, in the mass range $m_a = 5\text{--}90$ GeV.

2. The CMS detector

The central feature of the CMS apparatus is a superconducting solenoid of 6 m internal diameter, providing a magnetic field of 3.8 T. Within the solenoid volume are a silicon pixel and strip tracker, a lead tungstate crystal electromagnetic calorimeter (ECAL), and a brass and scintillator hadron calorimeter (HCAL), each composed of a barrel (EB and HB) and two endcap (EE and HE) sections. Forward calorimetry (HF), based on a steel absorber and quartz fibres that run longitudinally through the absorber and collect Cherenkov light, primarily from the electromagnetic particles, complements the coverage provided by the barrel and endcap detectors up to pseudorapidity $|\eta| = 5.2$. Muons are measured in gas-ionisation detectors embedded in the steel flux-return yoke outside the solenoid. The silicon tracker measures charged particles within the $|\eta| < 2.5$ range. It consists of 1440 silicon pixel and 15 148 silicon strip detector modules. For nonisolated charged particles in the transverse momentum range $1 < p_T < 10$ GeV and $|\eta| < 1.4$, the track resolutions are typically 1.5% in p_T and 25–90 (45–150) μm in the transverse (longitudinal) impact parameter [34]. The first level of the CMS trigger system [35], Level-1

(L1), composed of custom hardware processors, uses information from the calorimeters and muon detectors to select the most interesting events in a fixed time interval of less than 4 μs . The high-level trigger (HLT) processor farm further decreases the event rate before data storage. A more detailed description of the CMS detector, together with a definition of the coordinate system used and the relevant kinematic variables, can be found in Ref. [36].

3. Simulation and reconstruction

The light-by-light signal is generated with the MADGRAPH v5 [37] Monte Carlo (MC) event generator, with the modifications discussed in Refs. [7,38] to include the nuclear photon fluxes and the elementary LbL scattering process. The latter includes all quark and lepton loops at leading order, but omits the W boson contributions, which are only important for diphoton masses $m^{\gamma\gamma} > 2m_W$. Next-to-leading order (NLO) quantum chromodynamics and QED corrections increase $\sigma_{\gamma\gamma \rightarrow \gamma\gamma}$ by just a few percent [39] and are also neglected here. Exclusive $\gamma\gamma \rightarrow e^+e^-$ events can be misidentified as LbL scattering if neither electron track is reconstructed or if both electrons undergo hard bremsstrahlung. This QED process is generated using the STARLIGHT v2.76 [40,41] event generator, also based on the equivalent-photon fluxes. Since the cross section for the QED e^+e^- background is four to five orders of magnitude larger than that for LbL scattering, and it relies on physics objects (electrons) that are very similar to those of the signal (photons), the exclusive dielectron background is analysed in depth in order to estimate many of the (di)photon efficiencies directly from the data, as well as to determine an LbL/(QED e^+e^-) production cross sections ratio with reduced common uncertainties. The central exclusive production process, $gg \rightarrow \gamma\gamma$, is simulated using SUPERCHIC 2.0 [42], where the computed proton-proton cross section [26] is conservatively scaled to the PbPb case by multiplying it by $A^2 R_g^4$, where $A = 208$ is the mass number of lead and $R_g \approx 0.7$ is a gluon shadowing correction in the relevant kinematic range [43], and where the rapidity gap survival probability, encoding the probability to produce the diphoton system exclusively without any other hadronic activity, is assumed to be 100%. Given the large theoretical uncertainty of the CEP process for PbPb collisions, the absolute normalisation of this MC contribution is directly determined from a control region in the data, as explained later. All generated events are passed through the GEANT4 [44] detector simulation, and the events are reconstructed with the same software as for collision data. The simulation describes the tracker material budget with an accuracy better than 10%, as established by measuring the distribution of reconstructed nuclear interactions and photon conversions in the tracker [34,45].

Photons and electrons are reconstructed using an algorithm based on the particle flow global event description (GED) [46]. The GED algorithm uses information from each subdetector system to provide charged-particle tracks, calorimeter clusters, and muon tracks. Electromagnetic showers from photons and electrons

deposit 97% of their incident energy into an array of 5×5 ECAL crystals. The tracker material can induce photon conversion and electron bremsstrahlung and, because of the presence of the strong CMS solenoidal magnetic field, the energy reaching the calorimeter is thereby spread in ϕ . The spread energy is captured by building a cluster of clusters, or “supercluster” [47]. The GED algorithm allows for an almost complete recovery of the energy of the photons and electrons, even if they initiate an electromagnetic shower in the material in front of the ECAL. Nonetheless, in the case of photons, in order to keep to a minimum the e^\pm contamination, we require them to be unconverted in the tracker. The reconstructed energy of this supercluster is used to define the energy of the photon. Since the default CMS photon reconstruction algorithm is optimised for γ and e^\pm with transverse energies $E_T = E \sin\theta > 10$ GeV, whereas the cross section for photons and electrons from exclusive production peaks in the lower $E_T \approx 2$ –10 GeV range, a version of the GED algorithm optimised for this transverse energy range is employed. The threshold for the energy of photons, electrons, and superclusters, is lowered to 1 GeV, instead of the 10–15 GeV threshold used in the standard CMS analyses [47]. The full analysis is independently repeated using a different “hybrid” photon/electron reconstruction algorithm [47], obtaining reconstruction efficiencies and final results fully consistent with those derived with the default GED approach. Additional particle identification (ID) criteria are applied, in order to remove photons (mostly) from high- p_T neutral pion decays, based on a shower shape analysis that requires the width of the electromagnetic shower along the η direction to be below 0.02 (0.06) units in the ECAL barrel (endcap).

Electron candidates are identified by the association of a charged-particle track from the collision vertex with superclusters in the ECAL. The association takes into account energy deposits both from the electron and from bremsstrahlung photons produced during its passage through the inner detector. Additional electron identification criteria (isolation, number of tracker hits, HCAL/ECAL energy deposit) are applied, as discussed in Ref. [13]. The electron energy scale is verified using a sample of $\gamma\gamma \rightarrow e^+e^-$ events, comparing the energy of the supercluster E to the momentum of the track p . The electron E/p ratio is within 5% of unity in the barrel and 15% in the endcaps. A good agreement is found between data and simulation, both in the energy scale and resolution. In addition, the LbL simulation is also used to validate the photon energy scale. The reconstructed supercluster energy and generated photon energy agree within a few percent, confirming that the reconstructed supercluster energy is well calibrated.

4. Event selection and background estimation

The exclusive diphoton candidates are selected at the trigger level with a dedicated L1 algorithm that requires at least two electromagnetic clusters (L1 EG) with E_T above 2 GeV and at least one of the HF detectors with total energy below the noise threshold. No additional selection is applied in the HLT. Data are also recorded with single-photon triggers with E_T thresholds above 5 and 10 GeV, and used in this analysis to estimate the efficiency of the first trigger via a tag-and-probe procedure [48], as described below. In the offline analysis, events are selected with exactly two photons, each with $E_T > 2$ GeV and $|\eta| < 2.4$, that satisfy further selection requirements described below. Neutral and charged exclusivity selection criteria are applied to reject events having any additional activity over the range $|\eta| < 5.2$. First, all events with reconstructed charged-particle tracks with $p_T > 0.1$ GeV are removed from further analysis. Second, events are required to have no activity in the calorimeters, above energy noise thresholds (ranging between about 0.6 GeV in the barrel, to 4.9 GeV in the HF), outside a region $\Delta\eta < 0.15$ and $\Delta\phi < 0.7$ in the barrel ($\Delta\eta <$

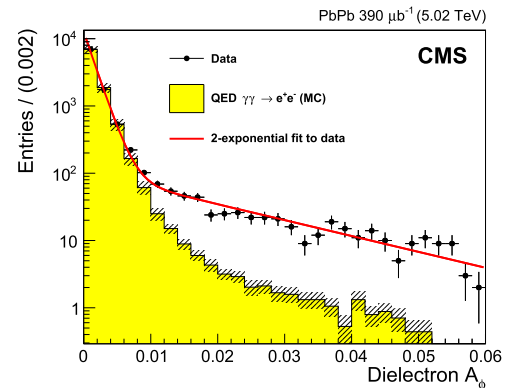


Fig. 2. Acoplanarity distribution of exclusive e^+e^- events measured in data (circles), compared to the expected QED e^+e^- spectrum in the STARLIGHT MC simulation (histogram), scaled as described in the text. The curve shows a χ^2 fit to the sum of two exponential distributions corresponding to exclusive e^+e^- plus any residual (nonacoplanar) background pairs. Error bars around the data points indicate statistical uncertainties, and hashed bands around the histogram include systematic and MC statistical uncertainties added in quadrature. The horizontal bars around the data symbols indicate the bin size.

0.15 and $\Delta\phi < 0.4$ in the endcap) around the two photons. The noise thresholds are determined from no- or single-bunch crossing events. To eliminate nonexclusive backgrounds, characterised by a final state with larger p_T and larger diphoton acoplanarities, $A_\phi = (1 - \Delta\phi^{\gamma\gamma}/\pi)$, than the back-to-back exclusive $\gamma\gamma$ events, the transverse momentum of the diphoton system is required to be $p_T^{\gamma\gamma} < 1$ GeV, and the acoplanarity of the pair to be $A_\phi < 0.01$. The chosen values of the pair p_T and acoplanarity selections, similar to those originally suggested in Ref. [7], are motivated by previous CMS studies of exclusive dilepton production [12–14]. The two dominant exclusive background sources potentially remaining in the LbL scattering signal region, $\gamma\gamma \rightarrow e^+e^-$ and CEP $gg \rightarrow \gamma\gamma$, are studied in detail next.

4.1. QED e^+e^- background

In order to have a full control of the QED e^+e^- background in the LbL scattering signal region, the same analysis carried out for the LbL events is done on exclusive dielectron candidates, applying the same criteria as described above for diphoton events, with the exception that exactly two opposite-sign electrons are reconstructed, instead of exactly two photons, and no additional track with $p_T > 0.1$ GeV should be present in addition to the two tracks corresponding to the electrons. Fig. 2 shows the acoplanarity distribution measured in QED e^+e^- events passing all selection criteria compared to the MC expectation.

The curve is a binned χ^2 fit of the data to the sum of two exponential functions representing the exclusive QED e^+e^- production plus any residual background in the high-acoplanarity tail. In the region of acoplanarity below 0.01, 9570 dielectron events are reconstructed with a purity of $\mathcal{P} = 0.960 \pm 0.002$ (stat), obtained from the ratio of amplitudes of the two exponential functions fitted to the data. The yellow histogram shows the same distribution obtained directly from the STARLIGHT MC simulation, scaled to the total number of events in data, multiplied by the purity. The corresponding kinematic distributions of the selected $\gamma\gamma \rightarrow e^+e^-$ events in the $A_\phi < 0.01$ region are shown in Fig. 3, together with the corresponding MC predictions normalised in the same manner. The hashed band around the MC histograms include the systematic uncertainties (trigger, electron reconstruction and identification, and MC statistical uncertainties added in quadrature) discussed in Section 6, estimated as a function of electron

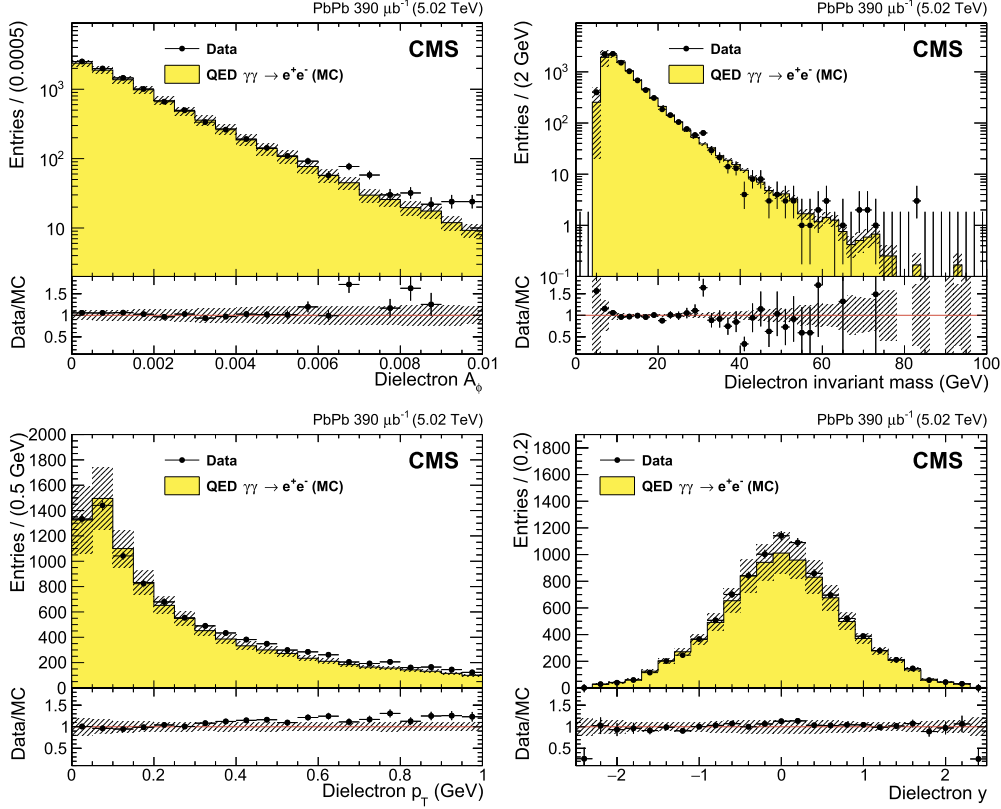


Fig. 3. Comparison of data (circles) and STARLIGHT MC expectation (histogram, scaled as described in the text) for the exclusive e^+e^- events passing all selection criteria, as a function of dielectron acoplanarity (top left), mass (top right), p_T (bottom left), and rapidity y (bottom right). Error bars around the data points indicate statistical uncertainties, and hashed bands around the histograms include systematic and MC statistical uncertainties added in quadrature. The horizontal bars around the data symbols indicate the bin size. The ratio of the data to the MC expectation is shown in the bottom panels.

E_T and η . A good data-to-simulation agreement is found, thereby confirming the quality of the electromagnetic particle reconstruction, and of the exclusive event selection criteria, as well as of the MC predictions [7,41] for exclusive particle production in ultraperipheral PbPb collisions at the LHC. Small systematic differences between the central values of the exclusive dielectron data and the MC prediction are seen in tails of some of the distributions (at increasing acoplanarity and p_T) due to the presence of slightly acoplanar events in data, likely from $\gamma\gamma \rightarrow e^+e^-$ events where one (or both) electrons radiate an extra soft photon, that are not explicitly simulated by the MC event generator. These small discrepancies have no impact on the final extracted cross sections integrated over the whole range of distribution(s).

The QED dielectron background is then directly estimated from the STARLIGHT MC simulation by counting the number of such e^+e^- events that pass all LbL scattering selection criteria. The charged exclusivity condition, requiring no track in the event above the $p_T = 0.1$ GeV threshold, is successful in removing this background almost entirely. This tracking efficiency is controlled in events with exactly two reconstructed photons and exactly one track, finding good data-MC agreement. The QED background in the signal region is estimated to be $N^{\text{ee,data}} = 1.0 \pm 0.3$ (stat) events, where the assigned uncertainty corresponds to the event count in the simulated samples.

4.2. Central exclusive diphoton background

Although the LbL and CEP processes share an identical final state, their kinematic distributions are different. Diphotons from quasireal $\gamma\gamma$ fusion processes are produced almost at rest in the

transverse plane and, thus, the final-state photons are emitted back-to-back with balanced pair transverse momentum $p_T^{\gamma\gamma} \approx 0$. On the other hand, typical CEP photon pairs are produced in diffractive-like gluon-mediated processes [26,42] with larger momentum exchanges leading to a diphoton transverse momentum distribution peaking at $p_T \approx 0.5$ GeV, after selection criteria, and moderately large tails in the azimuthal acoplanarity distribution. Thus, the requirement on diphoton acoplanarity ($A_\phi < 0.01$) also significantly reduces the $gg \rightarrow \gamma\gamma$ background. Since the MC prediction for CEP $gg \rightarrow \gamma\gamma$ has large theoretical uncertainties, and in order to account for any other remaining backgrounds resulting in photons that are not back-to-back (such as $\gamma\gamma \rightarrow e^+e^-\gamma(\gamma)$ events passing the analysis selection criteria), for which no event generator is currently available, the CEP background is normalised to match the data in the region $A_\phi > 0.02$, where the contribution from $\gamma\gamma \rightarrow \gamma\gamma$ is negligible (Fig. 4). The background normalisation factor is then obtained from

$$f_{\text{nonacoplanar}}^{\text{norm}} = \left[N_{\text{data}}(A_\phi > 0.02) - N_{\text{LbL}}^{\text{MC}}(A_\phi > 0.02) - N_{\text{QED}}^{\text{MC}}(A_\phi > 0.02) \right] / \left[N_{\text{CEP}}^{\text{MC}}(A_\phi > 0.02) \right], \quad (1)$$

and found to be $f_{\text{nonacoplanar}}^{\text{norm}} = 1.06 \pm 0.35$ (stat). The number of events due to CEP plus any residual backgrounds is thus estimated to be 3.0 ± 1.1 (stat). The statistical uncertainties quoted in both values are driven by the size of the data sample remaining at high acoplanarities, after all selection criteria have been applied.

Table 1

Number of diphoton candidates measured in data and expected from MC simulation for LbL scattering, QED e^+e^- production, and from the CEP+other contributions, after each event selection step (cumulative) described in the text. The yields of the simulated processes are scaled according to their theoretical cross sections and the integrated luminosity of the analysed data set. The CEP+other values are normalised from the high-acoplanarity tail with a scale factor estimated from the data as described in the text. The LbL scattering simulation uncertainty quoted is that of the theoretical uncertainty of the prediction, whereas the uncertainties in the QED e^+e^- and CEP+others yields are statistical.

Selection criteria	Data	LbL MC	QED e^+e^- MC	CEP MC+other (normalised to data)
Charged exclusivity	648	11.1 ± 1.2 (theo)	10.3 ± 1.0 (stat)	24.3 ± 8.1 (stat)
Neutral exclusivity	108	10.8 ± 1.1 (theo)	10.1 ± 1.0 (stat)	23.6 ± 7.9 (stat)
Diphoton $p_T < 1$ GeV	39	10.2 ± 1.1 (theo)	7.7 ± 1.0 (stat)	19.5 ± 6.5 (stat)
Diphoton acoplanarity < 0.01	14	9.0 ± 0.9 (theo)	1.0 ± 0.3 (stat)	3.0 ± 1.1 (stat)

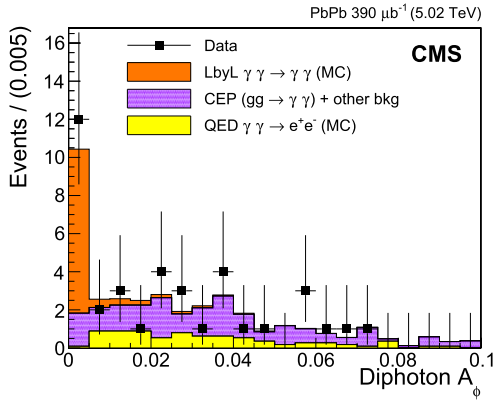


Fig. 4. Diphoton acoplanarity distribution for exclusive events measured in the data after selection criteria (squares), compared to the expected LbL scattering signal (orange histogram), QED e^+e^- (yellow histogram), and the CEP+other (light blue histogram, scaled to match the data in the $A_\phi > 0.02$ region as described in the text) backgrounds. Signal and QED e^+e^- MC samples are scaled according to their theoretical cross sections and integrated luminosity. The error bars around the data points indicate statistical uncertainties. The horizontal bars around the data symbols indicate the bin size.

4.3. Light-by-light signal distributions

The exclusive diphoton signal is extracted after applying all selection criteria described above and estimating the amount of residual QED e^+e^- and CEP+other backgrounds. Table 1 shows the number of events remaining after each selection criterion. The main selection requirement corresponds to two photons each with $E_T > 2$ GeV, $|\eta| < 2.4$ (excluding photons falling in the $\Delta\eta \approx 0.1$ gap region between the EB and EE, $1.444 < |\eta| < 1.566$), and diphoton invariant mass greater than 5 GeV. The numbers of events measured in data and expected from the sum of all MC contributions in the first two rows do not match because these selection requirements accept a fraction of nonexclusive backgrounds that are not included in the simulation. Once the full exclusivity selection criteria are applied, the data-to-simulation agreement is very good. We observe 14 LbL scattering candidates, to be compared with 9.0 ± 0.9 (theo) expected from the LbL scattering signal, 3.0 ± 1.1 (stat) from central exclusive plus any residual diphoton backgrounds, and 1.0 ± 0.3 (stat) from misidentified QED e^+e^- events.

An extra selection criterion has been also studied by further requiring that the candidate LbL scattering events have no signal above the noise threshold in the pixel tracker layers. This more stringent selection is sensitive to charged particles down to ~ 40 MeV, and results in a number of reconstructed LbL scattering signal counts (and even more reduced QED backgrounds) consistent with the MC predictions. However, since the efficiency of such a tight selection is difficult to assess from a control region

in data, the default analysis is kept with the charged-particle track $p_T > 0.1$ GeV exclusivity requirement.

Fig. 5 shows the comparison of the measured and simulated photon transverse momentum, photon pseudorapidity, photon azimuthal angle, diphoton invariant mass, diphoton rapidity, and diphoton transverse momentum distributions. Both the measured yields and kinematic distributions are in accord with the combination of the LbL scattering signal plus QED e^+e^- and CEP+other background expectations.

5. Cross section extraction

Given the low signal yield available for an extraction of differential cross section distributions, an integrated fiducial cross section for LbL scattering above a diphoton mass $m^{\gamma\gamma} = 5$ GeV is calculated instead. The ratio R of cross sections of the light-by-light scattering over the QED e^+e^- processes is measured, thereby reducing the uncertainties related to trigger and reconstruction efficiencies, and integrated luminosity. Efficiency uncertainties partially cancel in the ratio, as described later, thanks to a similar selection applied to photons and to electrons; and the integrated luminosity dependence fully cancels out. The ratio R is defined as

$$R = \frac{\sigma_{\text{fid}}(\gamma\gamma \rightarrow \gamma\gamma)}{\sigma(\gamma\gamma \rightarrow e^+e^-, m^{e^+e^-} > 5 \text{ GeV})} = \frac{N^{\gamma\gamma,\text{data}} - N^{\gamma\gamma,\text{bkg}}}{C^{\gamma\gamma}} \frac{C^{ee} \text{Acc}^{ee}}{N^{ee,\text{data}} \mathcal{P}}. \quad (2)$$

Here $\sigma_{\text{fid}}(\gamma\gamma \rightarrow \gamma\gamma)$ is the LbL scattering fiducial cross section (i.e. passing all the aforementioned p_T , η , $m^{\gamma\gamma}$ kinematic selection criteria for the single photons and for the photon pair); $\sigma(\gamma\gamma \rightarrow e^+e^-, m^{e^+e^-} > 5 \text{ GeV})$ is the total cross section for the QED e^+e^- process for masses above 5 GeV; $\text{Acc}^{ee} = N^{\text{gen}}(p_T^{\text{gen}} > 2 \text{ GeV}, |\eta^{\text{gen}}| < 2.4, m^{e^+e^-} > 5 \text{ GeV}) / N^{\text{gen}}(m^{e^+e^-} > 5 \text{ GeV}) = 0.058 \pm 0.001$ (stat) is the dielectron acceptance for the fiducial single-electron kinematic selections determined from the STARLIGHT MC generator; $N^{\gamma\gamma,\text{data}}$ is the number of diphoton events passing the selection in data; $N^{\gamma\gamma,\text{bkg}}$ is the estimated number of background events passing all selection criteria; $N^{ee,\text{data}}$ is the number of dielectron events passing our selection in data; \mathcal{P} is the purity of the estimated fraction of QED e^+e^- signal among these dielectron events; and $C^{\gamma\gamma}$ and C^{ee} are the overall efficiency correction factors, for the $\gamma\gamma$ and e^+e^- selections, respectively, that are determined as discussed in the next section.

5.1. Diphoton analysis efficiencies

The $C^{\gamma\gamma}$ correction factor in Eq. (2) is obtained through the factorised expression

$$C^{\gamma\gamma} = \varepsilon^{\gamma\gamma} (\text{SF}^{\gamma,\text{reco+ID}})^2 (\text{SF}^{\gamma\gamma,\text{trig}}) (\text{SF}^{\text{ch.excl.}}) (\text{SF}^{\text{neut.excl.}}), \quad (3)$$

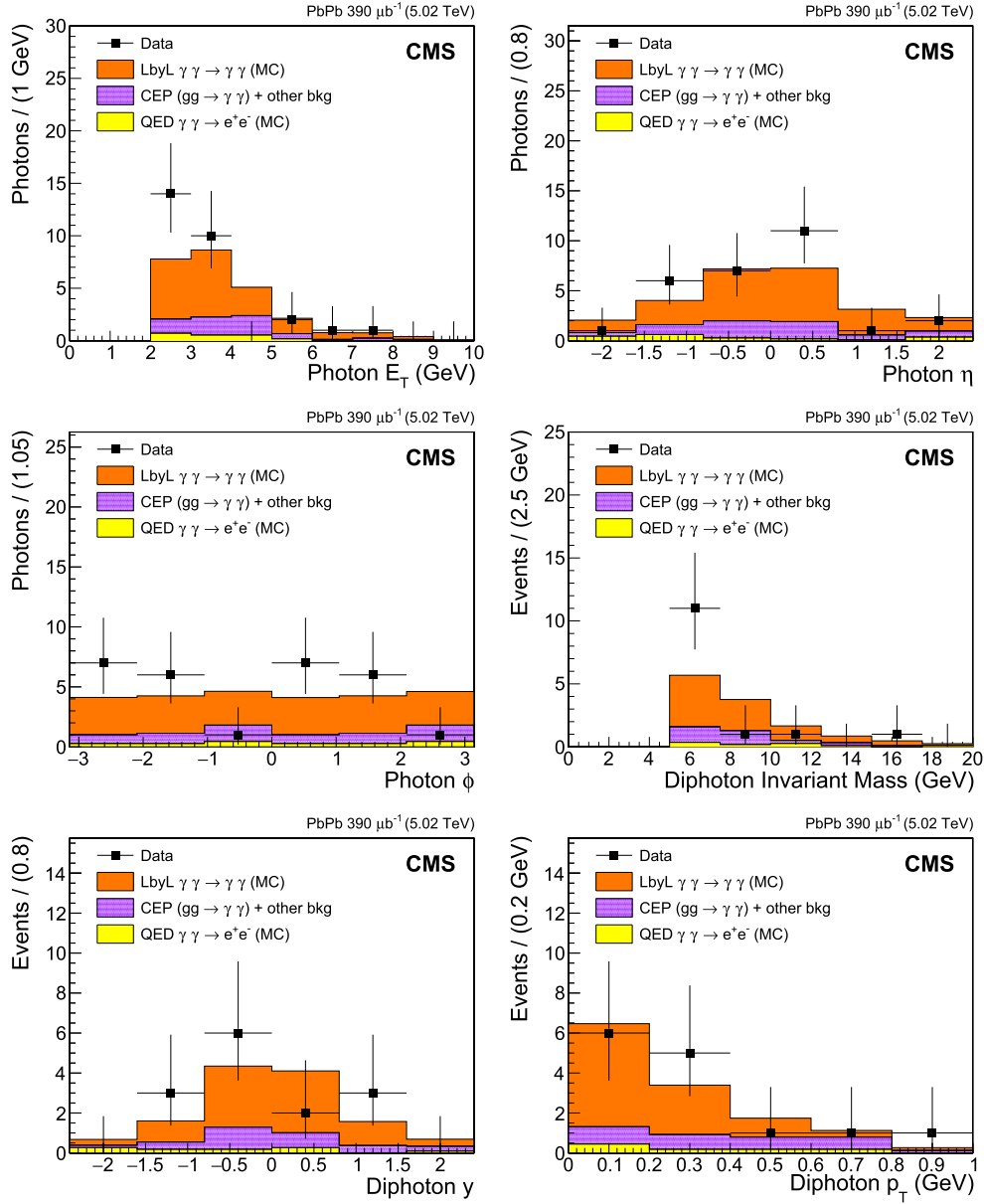


Fig. 5. Distributions of the single photon E_T , η , and ϕ , as well as diphoton p_T , rapidity, and invariant mass measured for the fourteen exclusive events passing all selection criteria (squares), compared to the expectations of LbL scattering signal (orange histogram), QED e^+e^- MC predictions (yellow histogram), and the CEP plus other backgrounds (light blue histogram, scaled to match the data in the $A_\phi > 0.02$ region). Signal and QED e^+e^- MC samples are scaled according to their theoretical cross sections and integrated luminosity. The error bars around the data points indicate statistical uncertainties. The horizontal bars around the data symbols indicate the bin size.

where the diphoton efficiency $\varepsilon^{\gamma\gamma}$ is determined using the LbL scattering MC simulation. This efficiency receives contributions from triggering, photon reconstruction and identification, and neutral and charged exclusivity criteria that are directly determined from the data via independent data-to-simulations scale factors, $SF = \varepsilon^{\text{data}} / \varepsilon^{\text{MC}}$, as explained below.

The diphoton efficiency is first derived from the LbL scattering simulation via:

$$\varepsilon^{\gamma\gamma} = \frac{N^{\text{reco}}(E_T > 2 \text{ GeV}, |\eta^{\text{reco}}| < 2.4, \text{ID, trigger, excl.})}{N^{\text{gen}}(E_T > 2 \text{ GeV}, |\eta^{\text{gen}}| < 2.4)}, \quad (4)$$

where the selection in the numerator and denominator applies to exactly two photons required in each event, which are also within the fiducial kinematic region in diphoton p_T , mass, and acoplanarity. It is found to be $\varepsilon^{\gamma\gamma} = (20.7 \pm 0.4)\%$, mostly driven by the inefficiencies of the single photon reconstruction and identi-

fication, and of the trigger ($\varepsilon^{\gamma, \text{reco+ID}}, \varepsilon^{\gamma\gamma, \text{trig.}} \approx 70\%$). The quoted uncertainty here is statistical only, reflecting the finite size of the LbL scattering MC sample.

The second term of Eq. (3), the photon reconstruction and identification efficiency correction ($SF^{\gamma, \text{reco+ID}}$), is extracted from data by selecting $\gamma\gamma \rightarrow e^+e^-(\gamma)$ events, where one of the electrons emits a hard bremsstrahlung photon due to interaction with the material of the tracker. The p_T of the two electrons in $\gamma\gamma \rightarrow e^+e^-$ events being approximately equal, if one of the electrons emits a hard bremsstrahlung photon, it may not reach the ECAL to be identified as an electron but it can still be reconstructed in the tracker as a charged particle.

In a first step, hard-bremsstrahlung events are selected among events passing a trigger requiring one L1 EG cluster with $E_T > 5$ GeV, that have exactly two oppositely charged particle tracks and exactly one electron reconstructed. Among those events,

we then look for exactly one photon compatible with a hard bremsstrahlung, as described below. Such events are used to estimate the efficiency in a tag-and-probe procedure, via

$$\varepsilon_{\text{data}}^{\gamma, \text{reco+ID, hard-brem}} = \frac{N_{\text{probe}}^{\text{reco+ID, hard-brem}}}{N_{\text{passing}}^{\text{reco+ID, hard-brem}}}, \quad (5)$$

where denominator and numerator are defined as follows:

- $N_{\text{passing}}^{\text{reco+ID, hard-brem}}$: Electrons are selected if (i) their direction matches with one of the two reconstructed tracks within a radius $\Delta R = \sqrt{(\Delta\eta)^2 + (\Delta\phi)^2} < 1.0$ (where η and ϕ are those of the electron track), (ii) they have E_T above 5 GeV, and (iii) their associated ECAL supercluster is matched within $\Delta R < 0.1$ to an L1 EG cluster with $E_T > 5$ GeV. The p_T of the track that is not matched with the electron should be below 2 GeV, since we assume that track to be generated by the electron after bremsstrahlung emission. The $p_T^{\text{unmatched track}} < 2$ GeV requirement ensures that this low- p_T charged particle is sufficiently bent by the magnetic field, and thus the expected photon (extrapolated to the ECAL) and the second electron are sufficiently separated. Events entering the denominator are not required to have a reconstructed photon.
- $N_{\text{probe}}^{\text{reco+ID, hard-brem}}$: Events from the denominator are also included in the numerator if a photon is found with $E_T > 2$ GeV that passes the identification criteria.

The efficiency is extracted using a fit to the acoplanarity distribution between the electron and the charged-particle track, and amounts to $\varepsilon_{\text{data}}^{\gamma, \text{reco+ID, hard-brem}} = (86.5 \pm 7.0)\%$, to be compared with $\varepsilon_{\text{MC}}^{\gamma, \text{reco+ID, hard-brem}} = (82.5 \pm 2.0)\%$ in the MC simulation, where uncertainties are statistical (as well as all other uncertainties quoted in this section). The ratio of these efficiencies is used to define the corresponding $\text{SF}^{\gamma, \text{reco+ID, hard-brem}} = 1.05 \pm 0.09$ scale factor. We note that this procedure checks not only the reconstruction and identification efficiency in data, but also effectively includes bin migrations outside the fiducial p_T range due to the effects of photon energy scale and resolution. The impact of bin migrations in the final diphoton cross section is found to be below the 1% level.

Events in the study above comprise exactly two charged-particle tracks, corresponding to the two electrons. They do not probe the possibility that the photon, reconstructed in the ECAL, has previously also interacted in the tracker generating an e^+e^- pair that has been also reconstructed as one or two additional displaced low- p_T charged-particle tracks. In the case of an LbL scattering event, such a genuine signal event would be discarded by the strict charged exclusivity criterion, which is applied independently of the proximity of the tracks to the photon, in order to keep the QED e^+e^- background to a minimum. The modeling of this efficiency loss in simulation is checked using hard-bremsstrahlung events with a similar selection as above, except that up to two additional charged-particle tracks are now allowed in the event. We check the fraction of events where no additional track, more displaced than the one with $p_T < 2$ GeV required in the selection, is found in a window $|\Delta\eta| < 0.15$, $|\Delta\phi| < 0.7$ around the photon. This efficiency amounts to $\varepsilon_{\text{data}}^{\gamma, \text{tk veto}} = (89.9 \pm 1.7)\%$ in data, and $\varepsilon_{\text{MC}}^{\gamma, \text{tk veto}} = (91.1 \pm 1.2)\%$ in the MC QED e^+e^- simulation. The ratio of these efficiencies gives $\text{SF}^{\gamma, \text{tk veto}} = 0.99 \pm 0.02$. The final overall scale factor for reconstruction and identification, accounting for the modeling of photon conversions in the MC simulation and the efficiency to reconstruct the associated displaced tracks, is then $\text{SF}^{\gamma, \text{reco+ID}} = \text{SF}^{\gamma, \text{reco+ID, hard-brem}} \text{SF}^{\gamma, \text{tk veto}} = 1.04 \pm 0.09$.

The third term of Eq. (3) accounts for the trigger selection efficiency. Exclusive diphoton events are selected using an L1 trigger requiring two electromagnetic clusters with $E_T > 2$ GeV, and no activity (above noise thresholds) in at least one of the HF calorimeters. These two components of the trigger, the electromagnetic cluster selection and the HF energy veto, are verified independently in data. The efficiency for reconstructing an L1 EG cluster with $E_T > 2$ GeV is verified using a tag-and-probe technique on QED e^+e^- events, where the dielectron acoplanarity is fitted to extract the signal and measure the efficiency. The same selection criteria used in the main analysis are applied, including the exclusivity requirements. Events are further selected using a supporting trigger requiring one L1 EG cluster with $E_T > 5$ GeV with the same HF energy veto as the analysis trigger. The L1 EG cluster used in the trigger is matched (using the same criterion mentioned above) to one of the two electrons reconstructed offline, called the tag. The other electron in the event is the probe, and it qualifies as a passing probe if it is matched to an L1 EG cluster with $E_T > 2$ GeV. The efficiency is then the fraction of probes that are also passing probes, and it is in the 45–100% range, with the lowest efficiency found close to the $E_T = 2$ GeV threshold and at high $|\eta|$. Scale factors are determined from the data-MC differences, as a function of E_T , in two $|\eta|$ bins. Applying them to the LbL simulation, we find an integrated scale factor of 1.12 ± 0.31 (stat). The same QED e^+e^- sample is used to test the HF veto component of the analysis trigger. This time, we apply the nominal dielectron selection, including exclusivity requirements, but for a data sample collected with a trigger requiring a single-EG object in the HLT with $E_T > 10$ GeV and $|\eta| < 1.5$ plus a small amount of energy in the HFs corresponding to about 50% of the most peripheral PbPb events. Both electrons in the event are then matched to an L1 EG cluster with $E_T > 2$ GeV. We find that $(100_{-3}^{+0})\%$ of the selected events also pass the analysis trigger, i.e. satisfy the HF veto in the trigger, in perfect agreement with the result predicted from the MC simulation. Combining the results of the studies above, the scale factor $\text{SF}^{\gamma\gamma, \text{trig}} = 1.12 \pm 0.31$ is obtained for the ratio of the product of trigger efficiencies in data to that obtained from the MC simulation.

The last two terms of Eq. (3) account for the efficiency of the exclusivity selections. The fraction of events passing the QED dielectron selection, with the exception of the charged and neutral exclusivity criteria, are analysed. Using the acoplanarity distribution to extract the signal, we find that $(92.5 \pm 0.3)\%$ of the events feature no additional track in the event, to be compared to $(99.3 \pm 0.1)\%$ in simulation. We deduce that the corresponding scale factor is $\text{SF}^{\text{ch.excl.}} = 0.93 \pm 0.01$. A similar strategy is used for the neutral exclusivity selection, this time in events passing the corresponding requirements. This efficiency is found to be $(89.9 \pm 1.4)\%$ in data, and $(96.9 \pm 1.3)\%$ in simulation. This scale factor is then $\text{SF}^{\text{neut.excl.}} = 0.93 \pm 0.02$. Differences between the exclusivity efficiencies in data and MC simulation are likely due to the presence of nonexclusive events, such as $\gamma\gamma \rightarrow e^+e^-$ processes with a small hadronic overlap of the lead ions, whose modeling is currently not available in the Monte Carlo generators. The incorporation of such nonexclusive events in the definition of the signal is irrelevant, because both $\text{SF}^{\text{ch.excl.}}$ and $\text{SF}^{\text{neut.excl.}}$ cancel out in the R ratio, as explained in Section 6.

5.2. Dielectron analysis efficiencies

For the exclusive dielectron analysis, the efficiency is estimated using the STARLIGHT MC simulation via

$$\varepsilon_{\text{ee}} = \frac{N^{\text{reco}}(p_T^{\text{reco}} > 2 \text{ GeV}, |\eta^{\text{reco}}| < 2.4, \text{ID, trigger, excl.})}{N^{\text{gen}}(p_T^{\text{gen}} > 2 \text{ GeV}, |\eta^{\text{gen}}| < 2.4)}, \quad (6)$$

Table 2

Summary of the overall cross section measurement efficiencies $C^{\gamma\gamma,ee}$, efficiencies from simulation $\varepsilon^{\gamma\gamma,ee}$, and individual data-to-simulation scale factors $SF^{\gamma\gamma,ee}$, obtained for the diphoton and dielectron analyses. ‘‘Reco. and ID’’ stands for reconstruction and identification. All quoted uncertainties are systematic.

Diphoton global efficiency, Eq. (3)	$C^{\gamma\gamma}$	=	$(21.5 \pm 6.5)\%$
Diphoton efficiency (from simulation)	$\varepsilon^{\gamma\gamma}$	=	$(20.7 \pm 0.4)\%$
γ reco. and ID data-to-simulation scale factor	$SF^{\gamma\gamma, \text{reco+ID}}$	=	1.04 ± 0.09
Diphoton trigger selection data-to-simulation scale factor	$SF^{\gamma\gamma, \text{trig.}}$	=	1.12 ± 0.31
Dielectron global efficiency, Eq. (7)	C^{ee}	=	$(9.4 \pm 1.5)\%$
Dielectron efficiency (simulation)	ε^{ee}	=	$(10.4 \pm 0.1)\%$
e^\pm reco. and ID data-to-simulation scale factor	$SF^{ee, \text{reco+ID}}$	=	0.98 ± 0.04
Dielectron trigger selection data-to-simulation scale factor	$SF^{ee, \text{e, trig.}}$	=	1.09 ± 0.16
Charged exclusivity data-to-simulation scale factor	$SF^{\text{ch.excl.}}$	=	0.93 ± 0.01
Neutral exclusivity data-to-simulation scale factor	$SF^{\text{neut.excl.}}$	=	0.93 ± 0.02

where the kinematic criteria in the numerator and denominator are applied to exactly the two electrons required in the event. The different components of the electron efficiency are again checked using data, via a factorised expression for the corresponding correction factors:

$$C^{ee} = \varepsilon^{ee} (SF^{e, \text{reco+ID}})^2 (SF^{ee, \text{trig.}}) (SF^{\text{ch.excl.}}) (SF^{\text{neut.excl.}}). \quad (7)$$

Most of the scale factors are common with those used in the diphoton analysis (since they are computed using the larger statistical sample of electrons in data), except for the reconstruction and identification efficiency, which we check again for electrons. For the latter, a tag-and-probe technique using a fit to the acoplanarity distribution in QED e^+e^- events is used, as done for the diphoton case, except that now the probe is a charged-particle track that is a passing probe if it is matched to an electron passing the reconstruction and identification criteria. We find an efficiency of $(89.4 \pm 1.2)\%$ in data, consistent with $(90.4 \pm 1.3)\%$ in the MC simulation, corresponding to a scale factor of $SF^{e, \text{reco+ID}} = 0.99 \pm 0.02$.

The scale factor for the trigger efficiency is also recomputed using the p_T spectrum in the QED e^+e^- MC simulation, using the same p_T - and $|\eta|$ -dependent scale factors as for $SF^{\gamma\gamma, \text{trig.}}$, leading to $SF^{ee, \text{trig.}} = 1.09 \pm 0.16$.

5.3. Summary of the efficiencies

The overall cross section measurement efficiencies, efficiencies in simulation, as well as the individual data-to-simulation scale factors, obtained for the diphoton and dielectron analyses are summarised in Table 2. Since the data-to-simulation scale factors are consistent with unity, they are not included in the numbers listed in Table 1 nor in the results plotted in Figs. 2–5, but they are used to obtain the results in Section 7. The overall diphoton cross section efficiency, Eq. (4), is about 20% compared with about 10% for dielectrons, Eq. (6). The dielectron analysis is a factor of two less efficient than the diphoton one, because each single electron has a relatively larger probability of losing energy by bremsstrahlung before reaching the ECAL, and therefore their probability to pass the trigger selection threshold and/or their energy be properly reconstructed is smaller. Such efficiency losses are further enhanced as they enter squared for two electrons to pass the trigger or be concurrently reconstructed above the p_T and mass thresholds.

6. Systematic uncertainties

The main sources of uncertainty in the LbL scattering and QED e^+e^- production measurements are related to the trigger and single γ, e^\pm reconstruction efficiencies (Table 2). The uncertainty in

Table 3

Summary of the systematic uncertainties in the ratio of the fiducial LbL scattering to total QED e^+e^- cross sections.

Photon reconstruction and identification ($SF^{\gamma, \text{reco+ID}}$)	$(2 \times 9)\%$
Electron reconstruction and identification ($SF^{e, \text{reco+ID}}$)	$(2 \times 2.5)\%$
Trigger	12%
Size of simulated background samples	6%
Total	23%

the latter is doubled in the total cross section, since we consider diphoton and dielectron final states. No additional uncertainty in the photon energy scale and resolution is considered, since possible data-simulation differences are already included in the derivation of the reconstruction and identification scale factors. Systematic uncertainties have been estimated for the different terms defining the ratio R of the LbL scattering over QED e^+e^- production cross sections given by Eq. (2), and are summarised in Table 3. Because the scale factors used for the trigger efficiency are common to the diphoton and dielectron analyses, their associated uncertainty cancels partially in the ratio. However, because of different reconstruction and identification efficiencies, the E_T spectrum of photons is different from that of the electrons, leading to only incomplete cancellation of the uncertainty. Assuming the uncertainty in each individual p_T -binned scale factor is fully correlated between the photon and electron cases, but with no correlation between the scale factors for different p_T , we propagate these uncertainties simultaneously to the numerator and denominator of the ratio $SF^{\gamma\gamma, \text{trigger}}/SF^{ee, \text{trigger}}$, resulting in a 12% uncertainty in that ratio. The charged and neutral exclusivity scale factors, common to the diphoton and dielectron measurements, are assumed to cancel in the ratio R . The rest of the SF terms listed in Table 2 have small statistical uncertainties from the finite size of the MC samples used to derive them, which propagate into percent uncertainties in the final cross section, and are neglected here.

Among the other parameters in Eq. (2), the normalisation of the CEP and QED e^+e^- backgrounds in the signal region propagates into a 16% uncertainty in the background yield (resulting in an 6% uncertainty in the cross section measurement), accounting for the finite size of the MC samples. An additional uncertainty of 25% (10% in the final cross section), reflecting the finite size of the data sample at high acoplanarities used for the absolute normalisation of the CEP plus residual nonexclusive backgrounds, is considered as a statistical uncertainty rather than a systematic one.

The final systematic uncertainty is obtained from adding in quadrature the individual uncertainties and is listed in the last row of Table 3.

7. Results

7.1. Light-by-light cross section

The compatibility of the data with the background-only hypothesis has been evaluated from the measured acoplanarity distribution (Fig. 4), using a profile-likelihood ratio as a test statistic, including all systematic uncertainties as nuisance parameters with log-normal priors [49,50]. The uncertainty due to the finite size of the MC samples is also included as an additional nuisance parameter for each bin of the histogram. The significance of the excess at low diphoton acoplanarity in data, estimated from the expected distribution of the test statistic for the background-only hypothesis obtained with pseudo-experiments, is 3.7 standard deviations (3.5 standard deviations expected). If using only the total number of events observed and expected in the region $A_\phi < 0.01$, we obtain a significance of 3.4 standard deviations (3.2 expected).

The final ratio of the fiducial LbL scattering to the total QED e^+e^- cross sections is obtained from Eq. (2), and amounts to

$$R = (25.0 \pm 9.6 \text{ (stat)} \pm 5.8 \text{ (syst)}) \times 10^{-6}, \quad (8)$$

where the statistical uncertainty includes the normalisation uncertainties of the CEP and QED backgrounds, added in quadrature. The fiducial cross section is obtained from the theoretical prediction of $\sigma(\gamma\gamma \rightarrow e^+e^-, m^{ee} > 5 \text{ GeV}) = 4.82 \pm 0.48$ (theo) mb from STARLIGHT, where the 10% uncertainty is derived from alternative approaches [51] to compute the nonhadronic-overlap condition in the simulation:

$$\sigma_{\text{fid}}(\gamma\gamma \rightarrow \gamma\gamma) = 120 \pm 46 \text{ (stat)} \pm 28 \text{ (syst)} \pm 12 \text{ (theo) nb}, \quad (9)$$

in good agreement with the theoretical LbL prediction [7] in the fiducial region, defined in Section 5, of

$$\sigma_{\text{fid}}(\gamma\gamma \rightarrow \gamma\gamma) = 116 \pm 12 \text{ nb}. \quad (10)$$

The 10% uncertainty in the LbL theoretical prediction covers different implementations of the nonhadronic-overlap condition computed with a Glauber model [52] for varying Pb radius and nucleon-nucleon cross section values, as well as neglected NLO corrections.

7.2. Exclusion limits on axion-like particle production

The measured invariant mass distribution (Fig. 5, center right) is used to search for possible narrow diphoton resonances, such as pseudoscalar axion-like particles produced in the process $\gamma\gamma \rightarrow a \rightarrow \gamma\gamma$ [30]. The LbL, QED, and CEP+other continuum processes are considered as backgrounds in this search. Fully simulated STARLIGHT samples for various ALP masses, m_a , ranging from 5 to 90 GeV are reconstructed with the same code used for the LbL analysis in order to estimate the ALP acceptance and efficiency, as well as the expected reconstructed diphoton mass template distributions. Corrections to the efficiency estimated in the MC simulation are derived based on data, and applied in the same way as for the LbL analysis. A binned maximum likelihood fit of the signal and background contributions is performed on the data, where systematic uncertainties are included as nuisance parameters with a log-normal prior. The CL_s criterion [53,54], with a profile likelihood ratio as test statistic [55], is used to extract exclusion limits in the $\sigma(\gamma\gamma \rightarrow a \rightarrow \gamma\gamma)$ cross section at 95% confidence level (CL). Limits on $\sigma(\gamma\gamma \rightarrow a \rightarrow \gamma\gamma)$ cross section for axion-like particles with masses 5–90 GeV are set in the 1500–20 nb range (Fig. 6). The 68 and 95% CL bands around the expected limits are obtained using pseudo-experiments.

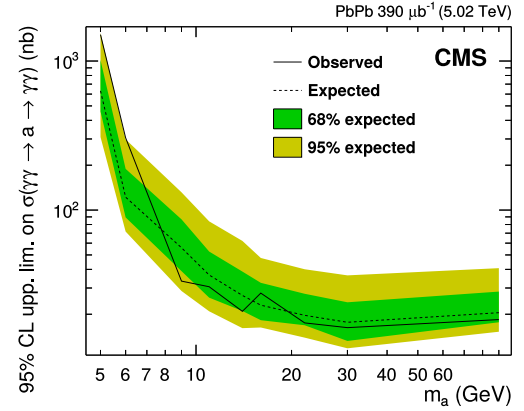


Fig. 6. Observed (full line) and expected (dotted line) 95% CL limits on the production cross section $\sigma(\gamma\gamma \rightarrow a \rightarrow \gamma\gamma)$ as a function of the ALP mass m_a in ultraperipheral PbPb collisions at $\sqrt{s_{NN}} = 5.02$ TeV. The inner (green) and outer (yellow) bands indicate the regions containing 68 and 95%, respectively, of the distribution of limits expected under the background-only hypothesis.

The cross section limits shown in Fig. 6 are used to set exclusion limits in the $g_{a\gamma}$ vs. m_a plane, where $g_{a\gamma} \equiv 1/\Lambda$ is the ALP coupling to photons (with Λ being the energy scale associated with the underlying U(1) symmetry whose spontaneous breaking generates the ALP mass). Two scenarios are considered where the ALP couples to photons $F^{\mu\nu}$ alone, or also to hypercharge $B^{\mu\nu}$ with operators: $a\tilde{F}\tilde{F}/4\Lambda$ and $aB\tilde{B}/(4\Lambda \cos^2 \theta_W)$ (where θ_W is the Weinberg angle), respectively [30]. The derived constraints on the ALP mass and its coupling to photons are compared in Fig. 7 to those obtained [30,56] from various experiments [13,57–59], assuming a 100% ALP decay branching fraction to diphotons. For an ALP sensitive to the electromagnetic current alone (left plot), our exclusion limits are the best so far over the $m_a = 5$ –50 GeV mass range. In the case of extra ALP couplings to electroweak currents (right plot), our result provides new constraints in the $m_a = 5$ –10 GeV region.

8. Summary

Evidence for light-by-light (LbL) scattering, $\gamma\gamma \rightarrow \gamma\gamma$, in ultraperipheral PbPb collisions at a centre-of-mass energy per nucleon pair of 5.02 TeV has been reported, based on a data sample corresponding to an integrated luminosity of $390 \mu\text{b}^{-1}$ recorded by the CMS experiment at the LHC in 2015. Fourteen LbL-scattering candidate events passing all selection requirements have been observed, with photon transverse energy above 2 GeV and pseudorapidity $|\eta| < 2.4$, diphoton invariant mass greater than 5 GeV, diphoton transverse momentum lower than 1 GeV, and diphoton acoplanarity below 0.01. Both the measured total yields and kinematic distributions are in accord with the expectations for the LbL scattering signal plus small residual backgrounds that are mostly from misidentified exclusive dielectron ($\gamma\gamma \rightarrow e^+e^-$) and gluon-induced central exclusive ($gg \rightarrow \gamma\gamma$) processes. The observed (expected) significance of the LbL scattering signal over the background-only expectation is 3.7 (3.5) standard deviations. The ratio of the fiducial LbL scattering to the total QED dielectron cross sections is $R = (25.0 \pm 9.6 \text{ (stat)} \pm 5.8 \text{ (syst)}) \times 10^{-6}$. From the theoretical $\gamma\gamma \rightarrow e^+e^-$ cross section prediction, we derive a fiducial light-by-light scattering cross section, $\sigma_{\text{fid}}(\gamma\gamma \rightarrow \gamma\gamma) = 120 \pm 46 \text{ (stat)} \pm 28 \text{ (syst)} \pm 12 \text{ (theo) nb}$, consistent with the standard model expectation. The measured exclusive diphoton invariant mass distribution is used to set new exclusion limits on the production of pseudoscalar axion-like particles (ALPs), via the process $\gamma\gamma \rightarrow a \rightarrow \gamma\gamma$, over the $m_a = 5$ –90 GeV mass range.

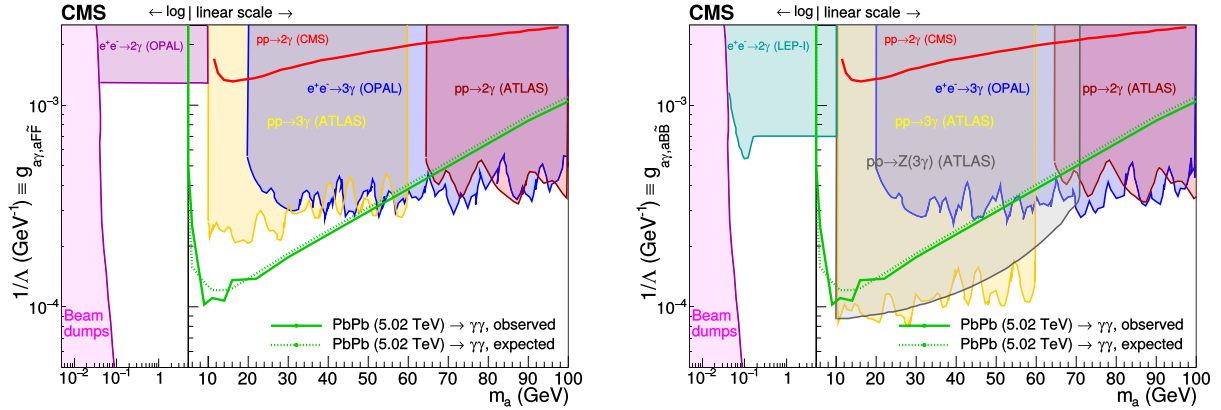


Fig. 7. Exclusion limits at 95% CL in the ALP-photon coupling $g_{\gamma\gamma}$ versus ALP mass m_a plane, for the operators $a\tilde{F}/4\Lambda$ (left, assuming ALP coupling to photons only) and $aB\tilde{B}/(4\Lambda\cos^2\theta_W)$ (right, including also the hypercharge coupling, thus processes involving the Z boson) derived in Refs. [30,56] from measurements at beam dumps [60], in e^+e^- collisions at LEP-I [56] and LEP-II [57], and in pp collisions at the LHC [13,58,59], and compared to the present PbPb limits.

For ALPs coupling to the electromagnetic (and electroweak) current, the derived exclusion limits are currently the best over the $m_a = 5\text{--}50$ GeV (5–10 GeV) mass range.

Acknowledgements

We congratulate our colleagues in the CERN accelerator departments for the excellent performance of the LHC and thank the technical and administrative staffs at CERN and at other CMS institutes for their contributions to the success of the CMS effort. In addition, we gratefully acknowledge the computing centres and personnel of the Worldwide LHC Computing Grid for delivering so effectively the computing infrastructure essential to our analyses. Finally, we acknowledge the enduring support for the construction and operation of the LHC and the CMS detector provided by the following funding agencies: BMBWF and FWF (Austria); FNRS and FWO (Belgium); CNPq, CAPES, FAPERJ, FAPERGS, and FAPESP (Brazil); MES (Bulgaria); CERN; CAS, MOST, and NSFC (China); COLCIENCIAS (Colombia); MSES and CSF (Croatia); RPF (Cyprus); SENESCYT (Ecuador); MoER, ERC IUT, and ERDF (Estonia); Academy of Finland, MEC, and HIP (Finland); CEA and CNRS/IN2P3 (France); BMBF, DFG, and HGF (Germany); GSRT (Greece); NKfIA (Hungary); DAE and DST (India); IPM (Iran); SFI (Ireland); INFN (Italy); MSIP and NRF (Republic of Korea); MES (Latvia); LAS (Lithuania); MOE and UM (Malaysia); BUAP, CINVESTAV, CONACYT, LNS, SEP, and UASLP-FAI (Mexico); MOS (Montenegro); MBIE (New Zealand); PAEC (Pakistan); MSHE and NSC (Poland); FCT (Portugal); JINR (Dubna); MON, ROSATOM, RAS, RFBR, and NRC KI (Russia); MESTD (Serbia); SEIDI, CPAN, PCTI, and FEDER (Spain); MoSTR (Sri Lanka); Swiss Funding Agencies (Switzerland); MST (Taipei); ThEPcenter, IPST, STAR, and NSTDA (Thailand); TUBITAK and TAEK (Turkey); NASU and SFFR (Ukraine); STFC (United Kingdom); DOE and NSF (USA).

Individuals have received support from the Marie-Curie programme and the European Research Council and Horizon 2020 Grant, contract No. 675440 (European Union); the Leventis Foundation; the Alfred P. Sloan Foundation; the Alexander von Humboldt Foundation; the Belgian Federal Science Policy Office; the Fonds pour la Formation à la Recherche dans l'Industrie et dans l'Agriculture (FRIA-Belgium); the Agentschap voor Innovatie door Wetenschap en Technologie (IWT-Belgium); the F.R.S. - FNRS and FWO (Belgium) under the “Excellence of Science - EOS” - be.h project n. 30820817; the Ministry of Education, Youth and Sports (MEYS) of the Czech Republic; the Lendület (“Momentum”) Programme and the János Bolyai Research Scholarship of the Hungarian Academy of Sciences, the New National Excellence Pro-

gram ÚNKP, the NKfIA research grants 123842, 123959, 124845, 124850 and 125105 (Hungary); the Council of Science and Industrial Research, India; the HOMING PLUS programme of the Foundation for Polish Science, cofinanced from European Union, Regional Development Fund, the Mobility Plus programme of the Ministry of Science and Higher Education, the National Science Center (Poland), contracts Harmonia 2014/14/M/ST2/00428, Opus 2014/13/B/ST2/02543, 2014/15/B/ST2/03998, and 2015/19/B/ST2/02861, Sonata-bis 2012/07/E/ST2/01406; the National Priorities Research Program by Qatar National Research Fund; the Programa Estatal de Fomento de la Investigación Científica y Técnica de Excelencia María de Maeztu, grant MDM-2015-0509 and the Programa Severo Ochoa del Principado de Asturias; the Thalís and Aristeia programmes cofinanced by EU-ESF and the Greek NSRF; the Rachadapisek Sompot Fund for Postdoctoral Fellowship, Chulalongkorn University and the Chulalongkorn Academic into Its 2nd Century Project Advancement Project (Thailand); the Welch Foundation, contract C-1845; and the Weston Havens Foundation (USA).

References

- [1] R.S. Van Dyck, P.B. Schwinberg, H.G. Dehmelt, New high precision comparison of electron and positron g-factors, *Phys. Rev. Lett.* 59 (1987) 26, <https://doi.org/10.1103/PhysRevLett.59.26>.
- [2] H.N. Brown, et al., Muon g-2, Precise measurement of the positive muon anomalous magnetic moment, *Phys. Rev. Lett.* 86 (2001) 2227, <https://doi.org/10.1103/PhysRevLett.86.2227>, arXiv:hep-ex/0102017.
- [3] A.I. Milstein, M. Schumacher, Present status of Delbrück scattering, *Phys. Rep.* 243 (1994) 183, [https://doi.org/10.1016/0370-1573\(94\)00058-1](https://doi.org/10.1016/0370-1573(94)00058-1).
- [4] S.L. Adler, Photon splitting and photon dispersion in a strong magnetic field, *Ann. Phys.* 67 (1971) 599, [https://doi.org/10.1016/0003-4916\(71\)90154-0](https://doi.org/10.1016/0003-4916(71)90154-0).
- [5] M. Bregant, et al., PVLAS, Limits on low energy photon-photon scattering from an experiment on magnetic vacuum birefringence, *Phys. Rev. D* 78 (2008) 032006, <https://doi.org/10.1103/PhysRevD.78.032006>, arXiv:0805.3036.
- [6] G. Jarlskog, L. Joansson, S. Pruenster, H.D. Schulz, H.J. Willutzki, G.G. Winter, Measurement of Delbrück scattering and observation of photon splitting at high energies, *Phys. Rev. D* 8 (1973) 3813, <https://doi.org/10.1103/PhysRevD.8.3813>.
- [7] D. d’Enterria, G.G. da Silva, Observing light-by-light scattering at the Large Hadron Collider, *Phys. Rev. Lett.* 111 (2013) 080405, <https://doi.org/10.1103/PhysRevLett.111.080405>, arXiv:1305.7142.
- [8] A.J. Baltz, et al., The physics of ultraperipheral collisions at the LHC, *Phys. Rep.* 458 (2008) 1, <https://doi.org/10.1016/j.physrep.2007.12.001>, arXiv:0706.3356.
- [9] C.F. von Weizsäcker, Radiation emitted in collisions of very fast electrons, *Z. Phys.* 88 (1934) 612, <https://doi.org/10.1007/BF01333110>.
- [10] E.J. Williams, Nature of the high-energy particles of penetrating radiation and status of ionization and radiation formulae, *Phys. Rev.* 45 (1934) 729, <https://doi.org/10.1103/PhysRev.45.729>.
- [11] E. Fermi, On the theory of collisions between atoms and electrically charged particles, *Nuovo Cimento* 2 (1925) 143, <https://doi.org/10.1007/BF02961914>, arXiv:hep-th/0205086.

- [12] CMS Collaboration, Exclusive photon-photon production of muon pairs in proton-proton collisions at $\sqrt{s} = 7$ TeV, *J. High Energy Phys.* 01 (2012) 052, [https://doi.org/10.1007/JHEP01\(2012\)052](https://doi.org/10.1007/JHEP01(2012)052), arXiv:1111.5536.
- [13] CMS Collaboration, Search for exclusive or semi-exclusive photon pair production and observation of exclusive and semi-exclusive electron pair production in pp collisions at $\sqrt{s} = 7$ TeV, *J. High Energy Phys.* 11 (2012) 080, [https://doi.org/10.1007/JHEP11\(2012\)080](https://doi.org/10.1007/JHEP11(2012)080), arXiv:1209.1666.
- [14] CMS and TOTEM Collaborations, Observation of proton-tagged, central (semi)exclusive production of high-mass lepton pairs in pp collisions at 13 TeV with the CMS-TOTEM precision proton spectrometer, *J. High Energy Phys.* 07 (2018) 153, [https://doi.org/10.1007/JHEP07\(2018\)153](https://doi.org/10.1007/JHEP07(2018)153), arXiv:1803.04496.
- [15] ALICE Collaboration, Coherent J/ψ photoproduction in ultra-peripheral Pb-Pb collisions at $\sqrt{s_{NN}} = 2.76$ TeV, *Phys. Lett. B* 718 (2013) 1273, <https://doi.org/10.1016/j.physletb.2012.11.059>, arXiv:1209.3715.
- [16] ALICE Collaboration, Charmonium and e^+e^- pair photoproduction at mid-rapidity in ultra-peripheral Pb-Pb collisions at $\sqrt{s_{NN}} = 2.76$ TeV, *Eur. Phys. J. C* 73 (2013) 2617, <https://doi.org/10.1140/epjc/s10052-013-2617-1>, arXiv:1305.1467.
- [17] ALICE Collaboration, Exclusive J/ψ photoproduction off protons in ultra-peripheral p-Pb collisions at $\sqrt{s_{NN}} = 5.02$ TeV, *Phys. Rev. Lett.* 113 (2014) 232504, <https://doi.org/10.1103/PhysRevLett.113.232504>, arXiv:1406.7819.
- [18] ATLAS Collaboration, Measurement of exclusive $\gamma\gamma \rightarrow e^+e^-$ production in proton-proton collisions at $\sqrt{s} = 7$ TeV with the ATLAS detector, *Phys. Lett. B* 749 (2015) 242, <https://doi.org/10.1016/j.physletb.2015.07.069>, arXiv:1506.07098.
- [19] ATLAS Collaboration, Measurement of the exclusive $\gamma\gamma \rightarrow \mu^+\mu^-$ process in proton-proton collisions at $\sqrt{s} = 13$ TeV with the ATLAS detector, *Phys. Lett. B* 777 (2018) 303, <https://doi.org/10.1016/j.physletb.2017.12.043>, arXiv:1708.04053.
- [20] LHCb Collaboration, Exclusive J/ψ and $\Psi(2S)$ production in pp collisions at $\sqrt{s} = 7$ TeV, *J. Phys. G* 40 (2013) 045001, <https://doi.org/10.1088/0954-3899/40/4/045001>, arXiv:1301.7084.
- [21] LHCb Collaboration, Updated measurements of exclusive J/ψ and $\Psi(2S)$ production cross-sections in pp collisions at $\sqrt{s} = 7$ TeV, *J. Phys. G* 41 (2014) 055002, <https://doi.org/10.1088/0954-3899/41/5/055002>, arXiv:1401.3288.
- [22] CMS Collaboration, Study of exclusive two-photon production of W^+W^- in pp collisions at $\sqrt{s} = 7$ TeV and constraints on anomalous quartic gauge couplings, *J. High Energy Phys.* 07 (2013) 116, [https://doi.org/10.1007/JHEP07\(2013\)116](https://doi.org/10.1007/JHEP07(2013)116), arXiv:1305.5596.
- [23] CMS Collaboration, Evidence for exclusive $\gamma\gamma \rightarrow W^+W^-$ production and constraints on anomalous quartic gauge couplings in pp collisions at $\sqrt{s} = 7$ and 8 TeV, *J. High Energy Phys.* 08 (2016) 119, [https://doi.org/10.1007/JHEP08\(2016\)119](https://doi.org/10.1007/JHEP08(2016)119), arXiv:1604.04464.
- [24] ATLAS Collaboration, Measurement of exclusive $\gamma\gamma \rightarrow W^+W^-$ production and search for exclusive Higgs boson production in pp collisions at $\sqrt{s} = 8$ TeV using the ATLAS detector, *Phys. Rev. D* 94 (2016) 032011, <https://doi.org/10.1103/PhysRevD.94.032011>, arXiv:1607.03745.
- [25] ATLAS Collaboration, Evidence for light-by-light scattering in heavy-ion collisions with the ATLAS detector at the LHC, *Nat. Phys.* 13 (2017) 852, <https://doi.org/10.1038/nphys4208>, arXiv:1702.01625.
- [26] V.A. Khoze, A.D. Martin, M.G. Ryskin, W.J. Stirling, Diffractive $\gamma\gamma$ production at hadron colliders, *Eur. Phys. J. C* 38 (2005) 475, <https://doi.org/10.1140/epjc/s2004-02059-0>, arXiv:hep-ph/0409037.
- [27] I.F. Ginzburg, A. Schiller, Search for a heavy magnetic monopole at the Tevatron and CERN LHC, *Phys. Rev. D* 57 (1998) 6599, <https://doi.org/10.1103/PhysRevD.57.R6599>, arXiv:hep-ph/9802310.
- [28] S. Fichtel, G. von Gersdorff, B. Lenzi, C. Royon, M. Saimpert, Light-by-light scattering with intact protons at the LHC: from standard model to new physics, *J. High Energy Phys.* 02 (2015) 165, [https://doi.org/10.1007/JHEP02\(2015\)165](https://doi.org/10.1007/JHEP02(2015)165), arXiv:1411.6629.
- [29] S. Fichtel, Shining light on polarizable dark particles, *J. High Energy Phys.* 04 (2017) 088, [https://doi.org/10.1007/JHEP04\(2017\)088](https://doi.org/10.1007/JHEP04(2017)088), arXiv:1609.01762.
- [30] S. Knapen, T. Lin, H.K. Lou, T. Melia, Searching for axionlike particles with ultraperipheral heavy-ion collisions, *Phys. Rev. Lett.* 118 (2017) 171801, <https://doi.org/10.1103/PhysRevLett.118.171801>, arXiv:1607.06083.
- [31] H. Sun, Large extra dimension effects through light-by-light scattering at the CERN LHC, *Eur. Phys. J. C* 74 (2014) 2977, <https://doi.org/10.1140/epjc/s10052-014-2977-1>, arXiv:1406.3897.
- [32] J. Ellis, N.E. Mavromatos, T. You, Light-by-light scattering constraint on Born-Infeld theory, *Phys. Rev. Lett.* 118 (2017) 261802, <https://doi.org/10.1103/PhysRevLett.118.261802>, arXiv:1703.08450.
- [33] E. Chapon, C. Royon, O. Kepka, Anomalous quartic $WW\gamma\gamma$, $ZZ\gamma\gamma$, and trilinear $WW\gamma$ couplings in two-photon processes at high luminosity at the LHC, *Phys. Rev. D* 81 (2010) 074003, <https://doi.org/10.1103/PhysRevD.81.074003>, arXiv:0912.5161.
- [34] CMS Collaboration, Description and performance of track and primary-vertex reconstruction with the CMS tracker, *J. Instrum.* 9 (2014) P10009, <https://doi.org/10.1088/1748-0221/9/10/P10009>, arXiv:1405.6569.
- [35] CMS Collaboration, The CMS trigger system, *J. Instrum.* 12 (2017) P01020, <https://doi.org/10.1088/1748-0221/12/01/P01020>, arXiv:1609.02366.
- [36] CMS Collaboration, The CMS experiment at the CERN LHC, *J. Instrum.* 3 (2008) S08004, <https://doi.org/10.1088/1748-0221/3/08/S08004>.
- [37] J. Alwall, R. Frederix, S. Frixione, V. Hirschi, F. Maltoni, O. Mattelaer, H.-S. Shao, T. Stelzer, P. Torrielli, M. Zaro, The automated computation of tree-level and next-to-leading order differential cross sections, and their matching to parton shower simulations, *J. High Energy Phys.* 07 (2014) 079, [https://doi.org/10.1007/JHEP07\(2014\)079](https://doi.org/10.1007/JHEP07(2014)079), arXiv:1405.0301.
- [38] D. d'Enterria, J.-P. Lansberg, Study of Higgs boson production and its $b\bar{b}$ decay in $\gamma\gamma$ processes in proton-nucleus collisions at the LHC, *Phys. Rev. D* 81 (2010) 014004, <https://doi.org/10.1103/PhysRevD.81.014004>, arXiv:0909.3047.
- [39] Z. Bern, A. De Freitas, L.J. Dixon, A. Ghinculov, H.L. Wong, QCD and QED corrections to light by light scattering, *J. High Energy Phys.* 11 (2001) 031, <https://doi.org/10.1088/1126-6708/2001/11/031>, arXiv:hep-ph/0109079.
- [40] S.R. Klein, J. Nystrand, Photoproduction of quarkonium in proton-proton and nucleus-nucleus collisions, *Phys. Rev. Lett.* 92 (2004) 142003, <https://doi.org/10.1103/PhysRevLett.92.142003>, arXiv:hep-ex/0311164.
- [41] S.R. Klein, J. Nystrand, J. Seger, Y. Gorunov, J. Butterworth, STARlight: a Monte Carlo simulation program for ultra-peripheral collisions of relativistic ions, *Comput. Phys. Commun.* 212 (2017) 258, <https://doi.org/10.1016/j.cpc.2016.10.016>, arXiv:1607.03838.
- [42] L.A. Harland-Lang, V.A. Khoze, M.G. Ryskin, Exclusive physics at the LHC with SuperChic 2, *Eur. Phys. J. C* 76 (2016) 9, <https://doi.org/10.1140/epjc/s10052-015-3832-8>, arXiv:1508.02718.
- [43] K.J. Eskola, P. Paakkinen, H. Paukkunen, C.A. Salgado, EPPS16: nuclear parton distributions with LHC data, *Eur. Phys. J. C* 77 (2017) 163, <https://doi.org/10.1140/epjc/s10052-017-4725-9>, arXiv:1612.05741.
- [44] S. Agostinelli, et al., GEANT4, GEANT4—a simulation toolkit, *Nucl. Instrum. Methods A* 506 (2003) 250, [https://doi.org/10.1016/S0168-9002\(03\)01368-8](https://doi.org/10.1016/S0168-9002(03)01368-8).
- [45] CMS Collaboration, Precision measurement of the structure of the CMS inner tracking system using nuclear interactions, *J. Instrum.* 13 (2018) P10034, <https://doi.org/10.1088/1748-0221/13/10/P10034>, arXiv:1807.03289.
- [46] CMS Collaboration, Particle-flow reconstruction and global event description with the CMS detector, *J. Instrum.* 12 (2017) P10003, <https://doi.org/10.1088/1748-0221/12/10/P10003>, arXiv:1706.04965.
- [47] CMS Collaboration, Performance of photon reconstruction and identification with the CMS detector in proton-proton collisions at $\sqrt{s} = 8$ TeV, *J. Instrum.* 10 (2015) P08010, <https://doi.org/10.1088/1748-0221/10/08/P08010>, arXiv:1502.02702.
- [48] CMS Collaboration, Measurements of inclusive W and Z cross sections in pp collisions at $\sqrt{s} = 7$ TeV, *J. High Energy Phys.* 01 (2011) 080, [https://doi.org/10.1007/JHEP01\(2011\)080](https://doi.org/10.1007/JHEP01(2011)080), arXiv:1012.2466.
- [49] R.J. Barlow, C. Beeston, Fitting using finite Monte Carlo samples, *Comput. Phys. Commun.* 77 (1993) 219, [https://doi.org/10.1016/0010-4655\(93\)90005-W](https://doi.org/10.1016/0010-4655(93)90005-W).
- [50] J.S. Conway, Incorporating nuisance parameters in likelihoods for multisource spectra, in: *Proceedings, PHYSTAT 2011 Workshop on Statistical Issues Related to Discovery Claims in Search Experiments and Unfolding*, CERN, Geneva, Switzerland, 17–20 January 2011, 2011, p. 115, arXiv:1103.0354.
- [51] L.A. Harland-Lang, V.A. Khoze, M.G. Ryskin, Exclusive LHC physics with heavy ions: SuperChic 3, *Eur. Phys. J. C* 79 (2019) 39, <https://doi.org/10.1140/epjc/s10052-018-6530-0>, arXiv:1810.06567.
- [52] C. Loizides, J. Kamin, D. d'Enterria, Improved Monte Carlo Glauber predictions at present and future nuclear colliders, *Phys. Rev. C* 97 (2018) 054910, <https://doi.org/10.1103/PhysRevC.97.054910>, arXiv:1710.07098.
- [53] T. Junk, Confidence level computation for combining searches with small statistics, *Nucl. Instrum. Methods A* 434 (1999) 435, [https://doi.org/10.1016/S0168-9002\(99\)00498-2](https://doi.org/10.1016/S0168-9002(99)00498-2), arXiv:hep-ex/9902006.
- [54] A.L. Read, Presentation of search results: the CL_s technique, *J. Phys. G* 28 (2002) 2693, <https://doi.org/10.1088/0954-3899/28/10/313>.
- [55] The ATLAS Collaboration, The CMS Collaboration, The LHC Higgs Combination Group, Procedure for the LHC Higgs Boson Search Combination in Summer 2011, Technical Report CMS-NOTE-2011-005, ATL-PHYS-PUB-2011-11, 2011, URL: <https://cds.cern.ch/record/1379837>.
- [56] J. Jaeckel, M. Spannowsky, Probing MeV to 90 GeV axion-like particles with LEP and LHC, *Phys. Lett. B* 753 (2016) 482, <https://doi.org/10.1016/j.physletb.2015.12.037>, arXiv:1509.00476.
- [57] G. Abbiendi, et al., OPAL, Multiphoton production in e^+e^- collisions at $\sqrt{s} = 181-209$ GeV, *Eur. Phys. J. C* 26 (2003) 331, <https://doi.org/10.1140/epjc/s2002-01074-5>, arXiv:hep-ex/0210016.
- [58] ATLAS Collaboration, Search for scalar diphoton resonances in the mass range 65–600 GeV with the ATLAS detector in pp collision data at $\sqrt{s} = 8$ TeV, *Phys. Rev. Lett.* 113 (2014) 171801, <https://doi.org/10.1103/PhysRevLett.113.171801>, arXiv:1407.6583.
- [59] ATLAS Collaboration, Search for new phenomena in events with at least three photons collected in pp collisions at $\sqrt{s} = 8$ TeV with the ATLAS detector, *Eur. Phys. J. C* 76 (2016) 210, <https://doi.org/10.1140/epjc/s10052-016-4034-8>, arXiv:1509.05051.
- [60] B. Döbrich, J. Jaeckel, F. Kahlhoefer, A. Ringwald, K. Schmidt-Hoberg, ALPtraum: ALP production in proton beam dump experiments, *J. High Energy Phys.* 02 (2016) 018, [https://doi.org/10.1007/JHEP02\(2016\)018](https://doi.org/10.1007/JHEP02(2016)018), arXiv:1512.03069.

The CMS Collaboration

A.M. Sirunyan, A. Tumasyan

Yerevan Physics Institute, Yerevan, Armenia

W. Adam, F. Ambroggi, E. Asilar, T. Bergauer, J. Brandstetter, M. Dragicevic, J. Erö, A. Escalante Del Valle, M. Flechl, R. Frühwirth¹, V.M. Ghete, J. Hrubec, M. Jeitler¹, N. Krammer, I. Krätschmer, D. Liko, T. Madlener, I. Mikulec, N. Rad, H. Rohringer, J. Schieck¹, R. Schöfbeck, M. Spanring, D. Spitzbart, A. Taurok, W. Waltenberger, J. Wittmann, C.-E. Wulz¹, M. Zarucki

Institut für Hochenergiephysik, Wien, Austria

V. Chekhovsky, V. Mossolov, J. Suarez Gonzalez

Institute for Nuclear Problems, Minsk, Belarus

E.A. De Wolf, D. Di Croce, X. Janssen, J. Lauwers, M. Pieters, H. Van Haevermaet, P. Van Mechelen, N. Van Remortel

Universiteit Antwerpen, Antwerpen, Belgium

S. Abu Zeid, F. Blekman, J. D'Hondt, I. De Bruyn, J. De Clercq, K. Deroover, G. Flouris, D. Lontkovskiy, S. Lowette, I. Marchesini, S. Moortgat, L. Moreels, Q. Python, K. Skovpen, S. Tavernier, W. Van Doninck, P. Van Mulders, I. Van Parijs

Vrije Universiteit Brussel, Brussel, Belgium

D. Beghin, B. Bilin, H. Brun, B. Clerbaux, G. De Lentdecker, H. Delannoy, B. Dorney, G. Fasanella, L. Favart, R. Goldouzian, A. Grebenyuk, A.K. Kalsi, T. Lenzi, J. Luetic, N. Postiau, E. Starling, L. Thomas, C. Vander Velde, P. Vanlaer, D. Vannerom, Q. Wang

Université Libre de Bruxelles, Bruxelles, Belgium

T. Cornelis, D. Dobur, A. Fagot, M. Gul, I. Khvastunov², D. Poyraz, C. Roskas, D. Trocino, M. Tytgat, W. Verbeke, B. Vermassen, M. Vit, N. Zaganidis

Ghent University, Ghent, Belgium

H. Bakhshiansohi, O. Bondu, S. Brochet, G. Bruno, C. Caputo, P. David, C. Delaere, M. Delcourt, B. Francois, A. Giammanco, G. Krintiras, V. Lemaître, A. Magitteri, A. Mertens, M. Musich, K. Piotrkowski, A. Saggio, M. Vidal Marono, S. Wertz, J. Zobec

Université Catholique de Louvain, Louvain-la-Neuve, Belgium

F.L. Alves, G.A. Alves, M. Correa Martins Junior, G. Correia Silva, C. Hensel, A. Moraes, M.E. Pol, P. Rebello Teles

Centro Brasileiro de Pesquisas Físicas, Rio de Janeiro, Brazil

E. Belchior Batista Das Chagas, W. Carvalho, J. Chinellato³, E. Coelho, E.M. Da Costa, G.G. Da Silveira⁴, D. De Jesus Damiao, C. De Oliveira Martins, S. Fonseca De Souza, H. Malbouisson, D. Matos Figueiredo, M. Melo De Almeida, C. Mora Herrera, L. Mundim, H. Nogima, W.L. Prado Da Silva, L.J. Sanchez Rosas, A. Santoro, A. Sznajder, M. Thiel, E.J. Tonelli Manganote³, F. Torres Da Silva De Araujo, A. Vilela Pereira

Universidade do Estado do Rio de Janeiro, Rio de Janeiro, Brazil

S. Ahuja^a, C.A. Bernardes^a, L. Calligaris^a, T.R. Fernandez Perez Tomei^a, E.M. Gregores^b, P.G. Mercadante^b, S.F. Novaes^a, Sandra S. Padula^a

^a Universidade Estadual Paulista, São Paulo, Brazil

^b Universidade Federal do ABC, São Paulo, Brazil

A. Aleksandrov, R. Hadjiiska, P. Iaydjiev, A. Marinov, M. Misheva, M. Rodozov, M. Shopova, G. Sultanov

Institute for Nuclear Research and Nuclear Energy, Bulgarian Academy of Sciences, Sofia, Bulgaria

A. Dimitrov, L. Litov, B. Pavlov, P. Petkov

University of Sofia, Sofia, Bulgaria

W. Fang⁵, X. Gao⁵, L. Yuan

Beihang University, Beijing, China

M. Ahmad, J.G. Bian, G.M. Chen, H.S. Chen, M. Chen, Y. Chen, C.H. Jiang, D. Leggat, H. Liao, Z. Liu, F. Romeo, S.M. Shaheen⁶, A. Spiezia, J. Tao, Z. Wang, E. Yazgan, H. Zhang, S. Zhang⁶, J. Zhao

Institute of High Energy Physics, Beijing, China

Y. Ban, G. Chen, A. Levin, J. Li, L. Li, Q. Li, Y. Mao, S.J. Qian, D. Wang, Z. Xu

State Key Laboratory of Nuclear Physics and Technology, Peking University, Beijing, China

Y. Wang

Tsinghua University, Beijing, China

C. Avila, A. Cabrera, C.A. Carrillo Montoya, L.F. Chaparro Sierra, C. Florez, C.F. González Hernández, M.A. Segura Delgado

Universidad de Los Andes, Bogota, Colombia

B. Courbon, N. Godinovic, D. Lelas, I. Puljak, T. Sculac

University of Split, Faculty of Electrical Engineering, Mechanical Engineering and Naval Architecture, Split, Croatia

Z. Antunovic, M. Kovac

University of Split, Faculty of Science, Split, Croatia

V. Brigljevic, D. Ferencek, K. Kadija, B. Mesic, A. Starodumov⁷, T. Susa

Institute Rudjer Boskovic, Zagreb, Croatia

M.W. Ather, A. Attikis, M. Kolosova, G. Mavromanolakis, J. Mousa, C. Nicolaou, F. Ptochos, P.A. Razis, H. Rykaczewski

University of Cyprus, Nicosia, Cyprus

M. Finger⁸, M. Finger Jr.⁸

Charles University, Prague, Czech Republic

E. Ayala

Escuela Politecnica Nacional, Quito, Ecuador

E. Carrera Jarrin

Universidad San Francisco de Quito, Quito, Ecuador

A. Ellithi Kamel⁹, M.A. Mahmoud^{10,11}, Y. Mohammed¹⁰

Academy of Scientific Research and Technology of the Arab Republic of Egypt, Egyptian Network of High Energy Physics, Cairo, Egypt

S. Bhowmik, A. Carvalho Antunes De Oliveira, R.K. Dewanjee, K. Ehataht, M. Kadastik, M. Raidal, C. Veelken

National Institute of Chemical Physics and Biophysics, Tallinn, Estonia

P. Eerola, H. Kirschenmann, J. Pekkanen, M. Voutilainen

Department of Physics, University of Helsinki, Helsinki, Finland

J. Havukainen, J.K. Heikkilä, T. Järvinen, V. Karimäki, R. Kinnunen, T. Lampén, K. Lassila-Perini, S. Laurila, S. Lehti, T. Lindén, P. Luukka, T. Mäenpää, H. Siikonen, E. Tuominen, J. Tuominiemi

Helsinki Institute of Physics, Helsinki, Finland

T. Tuuva

Lappeenranta University of Technology, Lappeenranta, Finland

M. Besancon, F. Couderc, M. Dejardin, D. Denegri, J.L. Faure, F. Ferri, S. Ganjour, A. Givernaud, P. Gras, G. Hamel de Monchenault, P. Jarry, C. Leloup, E. Locci, J. Malcles, G. Negro, J. Rander, A. Rosowsky, M.Ö. Sahin, M. Titov

IRFU, CEA, Université Paris-Saclay, Gif-sur-Yvette, France

A. Abdulsalam¹², C. Amendola, I. Antropov, F. Beaudette, P. Busson, C. Charlot, R. Granier de Cassagnac, I. Kucher, A. Lobanov, J. Martin Blanco, C. Martin Perez, M. Nguyen, C. Ochando, G. Ortona, P. Paganini, P. Pigard, J. Rembser, R. Salerno, J.B. Sauvan, Y. Sirois, A.G. Stahl Leitner, A. Zabi, A. Zghiche

Laboratoire Leprince-Ringuet, Ecole polytechnique, CNRS/IN2P3, Université Paris-Saclay, Palaiseau, France

J.-L. Agram¹³, J. Andrea, D. Bloch, J.-M. Brom, E.C. Chabert, V. Cherepanov, C. Collard, E. Conte¹³, J.-C. Fontaine¹³, D. Gelé, U. Goerlach, M. Jansová, A.-C. Le Bihan, N. Tonon, P. Van Hove

Université de Strasbourg, CNRS, IPHC UMR 7178, Strasbourg, France

S. Gadrat

Centre de Calcul de l'Institut National de Physique Nucleaire et de Physique des Particules, CNRS/IN2P3, Villeurbanne, France

S. Beauceron, C. Bernet, G. Boudoul, N. Chanon, R. Chierici, D. Contardo, P. Depasse, H. El Mamouni, J. Fay, L. Finco, S. Gascon, M. Gouzevitch, G. Grenier, B. Ille, F. Lagarde, I.B. Laktineh, H. Lattaud, M. Lethuillier, L. Mirabito, S. Perries, A. Popov¹⁴, V. Sordini, G. Touquet, M. Vander Donckt, S. Viret

Université de Lyon, Université Claude Bernard Lyon 1, CNRS-IN2P3, Institut de Physique Nucléaire de Lyon, Villeurbanne, France

T. Toriashvili¹⁵

Georgian Technical University, Tbilisi, Georgia

Z. Tsamalaidze⁸

Tbilisi State University, Tbilisi, Georgia

C. Autermann, L. Feld, M.K. Kiesel, K. Klein, M. Lipinski, M. Preuten, M.P. Rauch, C. Schomakers, J. Schulz, M. Teroerde, B. Wittmer, V. Zhukov¹⁴

RWTH Aachen University, I. Physikalisches Institut, Aachen, Germany

A. Albert, D. Duchardt, M. Endres, M. Erdmann, S. Ghosh, A. Güth, T. Hebbeker, C. Heidemann, K. Hoepfner, H. Keller, L. Mastrolorenzo, M. Merschmeyer, A. Meyer, P. Millet, S. Mukherjee, T. Pook, M. Radziej, H. Reithler, M. Rieger, A. Schmidt, D. Teyssier

RWTH Aachen University, III. Physikalisches Institut A, Aachen, Germany

G. Flügge, O. Hlushchenko, T. Kress, A. Künsken, T. Müller, A. Nehr Korn, A. Nowack, C. Pistone, O. Pooth, D. Roy, H. Sert, A. Stahl¹⁶

RWTH Aachen University, III. Physikalisches Institut B, Aachen, Germany

M. Aldaya Martin, T. Arndt, C. Asawatangtrakuldee, I. Babounikau, K. Beernaert, O. Behnke, U. Behrens, A. Bermúdez Martínez, D. Bertsche, A.A. Bin Anuar, K. Borras¹⁷, V. Botta, A. Campbell, P. Connor, C. Contreras-Campana, V. Danilov, A. De Wit, M.M. Defranchis, C. Diez Pados, D. Domínguez Damiani, G. Eckerlin, T. Eichhorn, A. Elwood, E. Eren, E. Gallo¹⁸, A. Geiser, A. Grohsjean, M. Guthoff, M. Haranko, A. Harb, J. Hauk, H. Jung, M. Kasemann, J. Keaveney, C. Kleinwort, J. Knolle, D. Krücker, W. Lange, A. Lelek, T. Lenz, J. Leonard, K. Lipka, W. Lohmann¹⁹, R. Mankel, I.-A. Melzer-Pellmann, A.B. Meyer, M. Meyer, M. Missiroli, G. Mittag, J. Mnich, V. Myronenko, S.K. Pflitsch, D. Pitzl, A. Raspereza, M. Savitskyi, P. Saxena, P. Schütze, C. Schwanenberger, R. Shevchenko, A. Singh, H. Tholen, O. Turkot, A. Vagnerini, G.P. Van Onsem, R. Walsh, Y. Wen, K. Wichmann, C. Wissing, O. Zenaiev

Deutsches Elektronen-Synchrotron, Hamburg, Germany

R. Aggleton, S. Bein, L. Benato, A. Benecke, V. Blobel, T. Dreyer, E. Garutti, D. Gonzalez, P. Gunnellini, J. Haller, A. Hinzmann, A. Karavdina, G. Kasieczka, R. Klanner, R. Kogler, N. Kovalchuk, S. Kurz, V. Kutzner, J. Lange, D. Marconi, J. Multhaupt, M. Niedziela, C.E.N. Niemeyer, D. Nowatschin, A. Perieanu, A. Reimers, O. Rieger, C. Scharf, P. Schleper, S. Schumann, J. Schwandt, J. Sonneveld, H. Stadie, G. Steinbrück, F.M. Stober, M. Stöver, A. Vanhoefer, B. Vormwald, I. Zoi

University of Hamburg, Hamburg, Germany

M. Akbiyik, C. Barth, M. Baselga, S. Baur, E. Butz, R. Caspart, T. Chwalek, F. Colombo, W. De Boer, A. Dierlamm, K. El Morabit, N. Faltermann, B. Freund, M. Giffels, M.A. Harrendorf, F. Hartmann¹⁶, S.M. Heindl, U. Husemann, F. Kassel¹⁶, I. Katkov¹⁴, S. Kudella, H. Mildner, S. Mitra, M.U. Mozer, Th. Müller, M. Plagge, G. Quast, K. Rabbertz, M. Schröder, I. Shvetsov, G. Sieber, H.J. Simonis, R. Ulrich, S. Wayand, M. Weber, T. Weiler, S. Williamson, C. Wöhrmann, R. Wolf

Karlsruher Institut fuer Technologie, Karlsruhe, Germany

G. Anagnostou, G. Daskalakis, T. Geralis, A. Kyriakis, D. Loukas, G. Paspalaki, I. Topsis-Giotis

Institute of Nuclear and Particle Physics (INPP), NCSR Demokritos, Aghia Paraskevi, Greece

G. Karathanasis, S. Kesisoglou, P. Kontaxakis, A. Panagiotou, I. Papavergou, N. Saoulidou, E. Tziaferi, K. Vellidis

National and Kapodistrian University of Athens, Athens, Greece

K. Kousouris, I. Papakrivopoulos, G. Tsipolitis

National Technical University of Athens, Athens, Greece

I. Evangelou, C. Foudas, P. Giannelios, P. Katsoulis, P. Kokkas, S. Mallios, N. Manthos, I. Papadopoulos, E. Paradas, J. Strologas, F.A. Triantis, D. Tsitsonis

University of Ioánnina, Ioánnina, Greece

M. Bartók²⁰, M. Csanad, N. Filipovic, P. Major, M.I. Nagy, G. Pasztor, O. Surányi, G.I. Veres

MTA-ELTE Lendület CMS Particle and Nuclear Physics Group, Eötvös Loránd University, Budapest, Hungary

G. Bencze, C. Hajdu, D. Horvath²¹, Á. Hunyadi, F. Sikler, T.Á. Vámi, V. Veszpremi, G. Vesztergombi[†]

Wigner Research Centre for Physics, Budapest, Hungary

N. Beni, S. Czellar, J. Karancsi²², A. Makovec, J. Molnar, Z. Szillasi

Institute of Nuclear Research ATOMKI, Debrecen, Hungary

P. Raics, Z.L. Trocsanyi, B. Ujvari

Institute of Physics, University of Debrecen, Debrecen, Hungary

S. Choudhury, J.R. Komaragiri, P.C. Tiwari

Indian Institute of Science (IISc), Bangalore, India

S. Bahinipati²³, C. Kar, P. Mal, K. Mandal, A. Nayak²⁴, D.K. Sahoo²³, S.K. Swain

National Institute of Science Education and Research, HBNI, Bhubaneswar, India

S. Bansal, S.B. Beri, V. Bhatnagar, S. Chauhan, R. Chawla, N. Dhingra, R. Gupta, A. Kaur, M. Kaur, S. Kaur, R. Kumar, P. Kumari, M. Lohan, A. Mehta, K. Sandeep, S. Sharma, J.B. Singh, A.K. Viridi, G. Walia

Panjab University, Chandigarh, India

A. Bhardwaj, B.C. Choudhary, R.B. Garg, M. Gola, S. Keshri, Ashok Kumar, S. Malhotra, M. Naimuddin, P. Priyanka, K. Ranjan, Aashaq Shah, R. Sharma

University of Delhi, Delhi, India

R. Bhardwaj²⁵, M. Bharti²⁵, R. Bhattacharya, S. Bhattacharya, U. Bhawandeep²⁵, D. Bhowmik, S. Dey, S. Dutt²⁵, S. Dutta, S. Ghosh, K. Mondal, S. Nandan, A. Purohit, P.K. Rout, A. Roy, S. Roy Chowdhury, G. Saha, S. Sarkar, M. Sharan, B. Singh²⁵, S. Thakur²⁵

Saha Institute of Nuclear Physics, HBNI, Kolkata, India

P.K. Behera

Indian Institute of Technology Madras, Madras, India

R. Chudasama, D. Dutta, V. Jha, V. Kumar, P.K. Netrakanti, L.M. Pant, P. Shukla

Bhabha Atomic Research Centre, Mumbai, India

T. Aziz, M.A. Bhat, S. Dugad, G.B. Mohanty, N. Sur, B. Sutar, Ravindra Kumar Verma

Tata Institute of Fundamental Research-A, Mumbai, India

S. Banerjee, S. Bhattacharya, S. Chatterjee, P. Das, M. Guchait, Sa. Jain, S. Karmakar, S. Kumar, M. Maity²⁶, G. Majumder, K. Mazumdar, N. Sahoo, T. Sarkar²⁶

Tata Institute of Fundamental Research-B, Mumbai, India

S. Chauhan, S. Dube, V. Hegde, A. Kapoor, K. Kothekar, S. Pandey, A. Rane, S. Sharma

Indian Institute of Science Education and Research (IISER), Pune, India

S. Chenarani²⁷, E. Eskandari Tadavani, S.M. Etesami²⁷, M. Khakzad, M. Mohammadi Najafabadi, M. Naseri, F. Rezaei Hosseinabadi, B. Safarzadeh²⁸, M. Zeinali

Institute for Research in Fundamental Sciences (IPM), Tehran, Iran

M. Felcini, M. Grunewald

University College Dublin, Dublin, Ireland

M. Abbrescia^{a,b}, C. Calabria^{a,b}, A. Colaleo^a, D. Creanza^{a,c}, L. Cristella^{a,b}, N. De Filippis^{a,c}, M. De Palma^{a,b}, A. Di Florio^{a,b}, F. Errico^{a,b}, L. Fiore^a, A. Gelmi^{a,b}, G. Iaselli^{a,c}, M. Ince^{a,b}, S. Lezki^{a,b}, G. Maggi^{a,c}, M. Maggi^a, G. Miniello^{a,b}, S. My^{a,b}, S. Nuzzo^{a,b}, A. Pompili^{a,b}, G. Pugliese^{a,c}, R. Radogna^a, A. Ranieri^a, G. Selvaggi^{a,b}, A. Sharma^a, L. Silvestris^a, R. Venditti^a, P. Verwilligen^a, G. Zito^a

^a INFN Sezione di Bari, Bari, Italy

^b Università di Bari, Bari, Italy

^c Politecnico di Bari, Bari, Italy

G. Abbiendi^a, C. Battilana^{a,b}, D. Bonacorsi^{a,b}, L. Borgonovi^{a,b}, S. Braibant-Giacomelli^{a,b}, R. Campanini^{a,b}, P. Capiluppi^{a,b}, A. Castro^{a,b}, F.R. Cavallo^a, S.S. Chhibra^{a,b}, C. Ciocca^a, G. Codispoti^{a,b}, M. Cuffiani^{a,b}, G.M. Dallavalle^a, F. Fabbri^a, A. Fanfani^{a,b}, E. Fontanesi, P. Giacomelli^a, C. Grandi^a, L. Guiducci^{a,b}, S. Lo Meo^a, S. Marcellini^a, G. Masetti^a, A. Montanari^a, F.L. Navarra^{a,b}, A. Perrotta^a, F. Primavera^{a,b,16}, A.M. Rossi^{a,b}, T. Rovelli^{a,b}, G.P. Siroli^{a,b}, N. Tosi^a

^a INFN Sezione di Bologna, Bologna, Italy

^b Università di Bologna, Bologna, Italy

S. Albergo^{a,b}, A. Di Mattia^a, R. Potenza^{a,b}, A. Tricomi^{a,b}, C. Tuve^{a,b}

^a INFN Sezione di Catania, Catania, Italy

^b Università di Catania, Catania, Italy

G. Barbagli^a, K. Chatterjee^{a,b}, V. Ciulli^{a,b}, C. Civinini^a, R. D'Alessandro^{a,b}, E. Focardi^{a,b}, G. Latino, P. Lenzi^{a,b}, M. Meschini^a, S. Paoletti^a, L. Russo^{a,29}, G. Sguazzoni^a, D. Strom^a, L. Viliani^a

^a INFN Sezione di Firenze, Firenze, Italy

^b Università di Firenze, Firenze, Italy

L. Benussi, S. Bianco, F. Fabbri, D. Piccolo

INFN Laboratori Nazionali di Frascati, Frascati, Italy

F. Ferro^a, F. Ravera^{a,b}, E. Robutti^a, S. Tosi^{a,b}

^a INFN Sezione di Genova, Genova, Italy

^b Università di Genova, Genova, Italy

A. Benaglia^a, A. Beschi^b, L. Brianza^{a,b}, F. Brivio^{a,b}, V. Ciriolo^{a,b,16}, S. Di Guida^{a,b,16}, M.E. Dinardo^{a,b}, S. Fiorendi^{a,b}, S. Gennai^a, A. Ghezzi^{a,b}, P. Govoni^{a,b}, M. Malberti^{a,b}, S. Malvezzi^a, A. Massironi^{a,b}, D. Menasce^a, F. Monti, L. Moroni^a, M. Paganoni^{a,b}, D. Pedrini^a, S. Ragazzi^{a,b}, T. Tabarelli de Fatis^{a,b}, D. Zuolo^{a,b}

^a INFN Sezione di Milano-Bicocca, Milano, Italy

^b Università di Milano-Bicocca, Milano, Italy

S. Buontempo^a, N. Cavallo^{a,c}, A. Di Crescenzo^{a,b}, F. Fabozzi^{a,c}, F. Fienga^a, G. Galati^a, A.O.M. Iorio^{a,b}, W.A. Khan^a, L. Lista^a, S. Meola^{a,d,16}, P. Paolucci^{a,16}, C. Sciacca^{a,b}, E. Voevodina^{a,b}

^a INFN Sezione di Napoli, Napoli, Italy

^b Università di Napoli 'Federico II', Napoli, Italy

^c Università della Basilicata, Potenza, Italy

^d Università G. Marconi, Roma, Italy

P. Azzi^a, N. Bacchetta^a, D. Bisello^{a,b}, A. Boletti^{a,b}, A. Bragagnolo, R. Carlin^{a,b}, P. Checchia^a, M. Dall'Osso^{a,b}, P. De Castro Manzano^a, T. Dorigo^a, U. Dosselli^a, F. Gasparini^{a,b}, U. Gasparini^{a,b}, A. Gozzelino^a, S.Y. Hoh, S. Lacaprara^a, P. Lujan, M. Margoni^{a,b}, A.T. Meneguzzo^{a,b}, J. Pazzini^{a,b}, P. Ronchese^{a,b}, R. Rossin^{a,b}, F. Simonetto^{a,b}, A. Tiko, E. Torassa^a, M. Zanetti^{a,b}, P. Zotto^{a,b}, G. Zumerle^{a,b}

^a INFN Sezione di Padova, Padova, Italy

^b Università di Padova, Padova, Italy

^c Università di Trento, Trento, Italy

A. Braghieri^a, A. Magnani^a, P. Montagna^{a,b}, S.P. Ratti^{a,b}, V. Re^a, M. Ressegotti^{a,b}, C. Riccardi^{a,b}, P. Salvini^a, I. Vai^{a,b}, P. Vitulo^{a,b}

^a INFN Sezione di Pavia, Pavia, Italy

^b Università di Pavia, Pavia, Italy

M. Biasini^{a,b}, G.M. Bilei^a, C. Cecchi^{a,b}, D. Ciangottini^{a,b}, L. Fanò^{a,b}, P. Lariccia^{a,b}, R. Leonardi^{a,b}, E. Manoni^a, G. Mantovani^{a,b}, V. Mariani^{a,b}, M. Menichelli^a, A. Rossi^{a,b}, A. Santocchia^{a,b}, D. Spiga^a

^a INFN Sezione di Perugia, Perugia, Italy

^b Università di Perugia, Perugia, Italy

K. Androsov^a, P. Azzurri^a, G. Bagliesi^a, L. Bianchini^a, T. Boccali^a, L. Borrello, R. Castaldi^a, M.A. Ciocci^{a,b}, R. Dell'Orso^a, G. Fedi^a, F. Fiori^{a,c}, L. Giannini^{a,c}, A. Giassi^a, M.T. Grippo^a, F. Ligabue^{a,c}, E. Manca^{a,c}, G. Mandorli^{a,c}, A. Messineo^{a,b}, F. Palla^a, A. Rizzi^{a,b}, P. Spagnolo^a, R. Tenchini^a, G. Tonelli^{a,b}, A. Venturi^a, P.G. Verdini^a

^a INFN Sezione di Pisa, Pisa, Italy

^b Università di Pisa, Pisa, Italy

^c Scuola Normale Superiore di Pisa, Pisa, Italy

L. Barone^{a,b}, F. Cavallari^a, M. Cipriani^{a,b}, D. Del Re^{a,b}, E. Di Marco^{a,b}, M. Diemoz^a, S. Gelli^{a,b}, E. Longo^{a,b}, B. Marzocchi^{a,b}, P. Meridiani^a, G. Organtini^{a,b}, F. Pandolfi^a, R. Paramatti^{a,b}, F. Preiato^{a,b}, S. Rahatlou^{a,b}, C. Rovelli^a, F. Santanastasio^{a,b}

^a INFN Sezione di Roma, Rome, Italy

^b Sapienza Università di Roma, Rome, Italy

N. Amapane^{a,b}, R. Arcidiacono^{a,c}, S. Argiro^{a,b}, M. Arneodo^{a,c}, N. Bartosik^a, R. Bellan^{a,b}, C. Biino^a, N. Cartiglia^a, F. Cenna^{a,b}, S. Cometti^a, M. Costa^{a,b}, R. Covarelli^{a,b}, N. Demaria^a, B. Kiani^{a,b}, C. Mariotti^a, S. Maselli^a, E. Migliore^{a,b}, V. Monaco^{a,b}, E. Monteil^{a,b}, M. Monteno^a, M.M. Obertino^{a,b}, L. Pacher^{a,b}, N. Pastrone^a, M. Pelliccioni^a, G.L. Pinna Angioni^{a,b}, A. Romero^{a,b}, M. Ruspa^{a,c}, R. Sacchi^{a,b}, K. Shchelina^{a,b}, V. Sola^a, A. Solano^{a,b}, D. Soldi^{a,b}, A. Staiano^a

^a INFN Sezione di Torino, Torino, Italy

^b Università di Torino, Torino, Italy

^c Università del Piemonte Orientale, Novara, Italy

S. Belforte^a, V. Candelise^{a,b}, M. Casarsa^a, F. Cossutti^a, A. Da Rold^{a,b}, G. Della Ricca^{a,b}, F. Vazzoler^{a,b}, A. Zanetti^a

^a INFN Sezione di Trieste, Trieste, Italy

^b Università di Trieste, Trieste, Italy

D.H. Kim, G.N. Kim, M.S. Kim, J. Lee, S. Lee, S.W. Lee, C.S. Moon, Y.D. Oh, S.I. Pak, S. Sekmen, D.C. Son, Y.C. Yang

Kyungpook National University, Daegu, Republic of Korea

H. Kim, D.H. Moon, G. Oh

Chonnam National University, Institute for Universe and Elementary Particles, Kwangju, Republic of Korea

J. Goh³⁰, T.J. Kim

Hanyang University, Seoul, Republic of Korea

S. Cho, S. Choi, Y. Go, D. Gyun, S. Ha, B. Hong, Y. Jo, K. Lee, K.S. Lee, S. Lee, J. Lim, S.K. Park, Y. Roh

Korea University, Seoul, Republic of Korea

H.S. Kim

Sejong University, Seoul, Republic of Korea

J. Almond, J. Kim, J.S. Kim, H. Lee, K. Lee, K. Nam, S.B. Oh, B.C. Radburn-Smith, S.h. Seo, U.K. Yang, H.D. Yoo, G.B. Yu

Seoul National University, Seoul, Republic of Korea

D. Jeon, H. Kim, J.H. Kim, J.S.H. Lee, I.C. Park

University of Seoul, Seoul, Republic of Korea

Y. Choi, C. Hwang, J. Lee, I. Yu

Sungkyunkwan University, Suwon, Republic of Korea

V. Dudenas, A. Juodagalvis, J. Vaitkus

Vilnius University, Vilnius, Lithuania

I. Ahmed, Z.A. Ibrahim, M.A.B. Md Ali³¹, F. Mohamad Idris³², W.A.T. Wan Abdullah, M.N. Yusli, Z. Zolkapli

National Centre for Particle Physics, Universiti Malaya, Kuala Lumpur, Malaysia

J.F. Benitez, A. Castaneda Hernandez, J.A. Murillo Quijada

Universidad de Sonora (UNISON), Hermosillo, Mexico

H. Castilla-Valdez, E. De La Cruz-Burelo, M.C. Duran-Osuna, I. Heredia-De La Cruz³³, R. Lopez-Fernandez, J. Mejia Guisao, R.I. Rabadan-Trejo, M. Ramirez-Garcia, G. Ramirez-Sanchez, R. Reyes-Almanza, A. Sanchez-Hernandez

Centro de Investigacion y de Estudios Avanzados del IPN, Mexico City, Mexico

S. Carrillo Moreno, C. Oropeza Barrera, F. Vazquez Valencia

Universidad Iberoamericana, Mexico City, Mexico

J. Eysermans, I. Pedraza, H.A. Salazar Ibarquen, C. Uribe Estrada

Benemerita Universidad Autonoma de Puebla, Puebla, Mexico

A. Morelos Pineda

Universidad Autónoma de San Luis Potosí, San Luis Potosí, Mexico

D. Krofcheck

University of Auckland, Auckland, New Zealand

S. Bheesette, P.H. Butler

University of Canterbury, Christchurch, New Zealand

A. Ahmad, M. Ahmad, M.I. Asghar, Q. Hassan, H.R. Hoorani, A. Saddique, M.A. Shah, M. Shoaib, M. Waqas

National Centre for Physics, Quaid-I-Azam University, Islamabad, Pakistan

H. Bialkowska, M. Bluj, B. Boimska, T. Frueboes, M. Górski, M. Kazana, K. Nawrocki, M. Szleper, P. Traczyk, P. Zalewski

National Centre for Nuclear Research, Swierk, Poland

K. Bunkowski, A. Byszuk³⁴, K. Doroba, A. Kalinowski, M. Konecki, J. Krolikowski, M. Misiura, M. Olszewski, A. Pyskir, M. Walczak

Institute of Experimental Physics, Faculty of Physics, University of Warsaw, Warsaw, Poland

M. Araujo, P. Bargassa, C. Beirão Da Cruz E Silva, A. Di Francesco, P. Faccioli, B. Galinhas, M. Gallinaro, J. Hollar, N. Leonardo, M.V. Nemallapudi, J. Seixas, G. Strong, O. Toldaiev, D. Vadrucchio, J. Varela

Laboratório de Instrumentação e Física Experimental de Partículas, Lisboa, Portugal

S. Afanasiev, P. Bunin, M. Gavrilenko, I. Golutvin, I. Gorbunov, A. Kamenev, V. Karjavine, A. Lanev, A. Malakhov, V. Matveev^{35,36}, P. Moisezenz, V. Palichik, V. Perelygin, S. Shmatov, S. Shulha, N. Skatchkov, V. Smirnov, N. Voytishin, A. Zarubin

Joint Institute for Nuclear Research, Dubna, Russia

V. Golovtsov, Y. Ivanov, V. Kim³⁷, E. Kuznetsova³⁸, P. Levchenko, V. Murzin, V. Oreshkin, I. Smirnov, D. Sosnov, V. Sulimov, L. Uvarov, S. Vavilov, A. Vorobyev

Petersburg Nuclear Physics Institute, Gatchina (St. Petersburg), Russia

Yu. Andreev, A. Dermenev, S. Gninenko, N. Golubev, A. Karneyeu, M. Kirsanov, N. Krasnikov, A. Pashenkov, D. Tlisov, A. Toropin

Institute for Nuclear Research, Moscow, Russia

V. Epshteyn, V. Gavrilov, N. Lychkovskaya, V. Popov, I. Pozdnyakov, G. Safronov, A. Spiridonov, A. Stepenov, V. Stolin, M. Toms, E. Vlasov, A. Zhokin

Institute for Theoretical and Experimental Physics, Moscow, Russia

T. Aushev

Moscow Institute of Physics and Technology, Moscow, Russia

M. Chadeeva³⁹, P. Parygin, D. Philippov, S. Polikarpov³⁹, E. Popova, V. Rusinov

National Research Nuclear University 'Moscow Engineering Physics Institute' (MEPhI), Moscow, Russia

V. Andreev, M. Azarkin³⁶, I. Dremin³⁶, M. Kirakosyan³⁶, S.V. Rusakov, A. Terkulov

P.N. Lebedev Physical Institute, Moscow, Russia

A. Baskakov, A. Belyaev, E. Boos, A. Ershov, A. Gribushin, L. Khein, V. Klyukhin, O. Kodolova, I. Lokhtin, O. Lukina, I. Miagkov, S. Obraztsov, S. Petrushanko, V. Savrin, A. Snigirev

Skobeltsyn Institute of Nuclear Physics, Lomonosov Moscow State University, Moscow, Russia

A. Barnyakov⁴⁰, V. Blinov⁴⁰, T. Dimova⁴⁰, L. Kardapoltsev⁴⁰, Y. Skovpen⁴⁰

Novosibirsk State University (NSU), Novosibirsk, Russia

I. Azhgirey, I. Bayshev, S. Bitioukov, D. Elumakhov, A. Godizov, V. Kachanov, A. Kalinin, D. Konstantinov, P. Mandrik, V. Petrov, R. Ryutin, S. Slabospitskii, A. Sobol, S. Troshin, N. Tyurin, A. Uzunian, A. Volkov

Institute for High Energy Physics of National Research Centre 'Kurchatov Institute', Protvino, Russia

A. Babaev, S. Baidali, V. Okhotnikov

National Research Tomsk Polytechnic University, Tomsk, Russia

P. Adzic⁴¹, P. Cirkovic, D. Devetak, M. Dordevic, J. Milosevic

University of Belgrade, Faculty of Physics and Vinca Institute of Nuclear Sciences, Belgrade, Serbia

J. Alcaraz Maestre, A. Álvarez Fernández, I. Bachiller, M. Barrio Luna, J.A. Brochero Cifuentes, M. Cerrada, N. Colino, B. De La Cruz, A. Delgado Peris, C. Fernandez Bedoya, J.P. Fernández Ramos, J. Flix, M.C. Fouz, O. Gonzalez Lopez, S. Goy Lopez, J.M. Hernandez, M.I. Josa, D. Moran, A. Pérez-Calero Yzquierdo, J. Puerta Pelayo, I. Redondo, L. Romero, M.S. Soares, A. Triossi

Centro de Investigaciones Energéticas Medioambientales y Tecnológicas (CIEMAT), Madrid, Spain

C. Albajar, J.F. de Trocóniz

Universidad Autónoma de Madrid, Madrid, Spain

J. Cuevas, C. Erice, J. Fernandez Menendez, S. Folgueras, I. Gonzalez Caballero, J.R. González Fernández, E. Palencia Cortezon, V. Rodríguez Bouza, S. Sanchez Cruz, P. Vischia, J.M. Vizán Garcia

Universidad de Oviedo, Oviedo, Spain

I.J. Cabrillo, A. Calderon, B. Chazin Quero, J. Duarte Campderros, M. Fernandez, P.J. Fernández Manteca, A. García Alonso, J. Garcia-Ferrero, G. Gomez, A. Lopez Virto, J. Marco, C. Martinez Rivero, P. Martinez Ruiz del Arbol, F. Matorras, J. Piedra Gomez, C. Prieels, T. Rodrigo, A. Ruiz-Jimeno, L. Scodellaro, N. Trevisani, I. Vila, R. Vilar Cortabitarte

Instituto de Física de Cantabria (IFCA), CSIC-Universidad de Cantabria, Santander, Spain

N. Wickramage

University of Ruhuna, Department of Physics, Matara, Sri Lanka

D. Abbaneo, B. Akgun, E. Auffray, G. Auzinger, P. Baillon, A.H. Ball, D. Barney, J. Bendavid, M. Bianco, A. Bocci, C. Botta, E. Brondolin, T. Camporesi, M. Cepeda, G. Cerminara, E. Chapon, Y. Chen, G. Cucciati, D. d'Enterria, A. Dabrowski, N. Daci, V. Daponte, A. David, A. De Roeck, N. Deelen, M. Dobson, M. Dünser, N. Dupont, A. Elliott-Peisert, P. Everaerts, F. Fallavollita⁴², D. Fasanella, G. Franzoni, J. Fulcher, W. Funk, D. Gigi, A. Gilbert, K. Gill, F. Glege, M. Guilbaud, D. Gulhan, J. Hegeman, C. Heidegger, V. Innocente, A. Jafari, P. Janot, O. Karacheban¹⁹, J. Kieseler, A. Kornmayer, M. Krammer¹, C. Lange, P. Lecoq, C. Lourenço, L. Malgeri, M. Mannelli, F. Meijers, J.A. Merlin, S. Mersi, E. Meschi, P. Milenovic⁴³, F. Moortgat, M. Mulders, J. Ngadiuba, S. Nourbakhsh, S. Orfanelli, L. Orsini, F. Pantaleo¹⁶, L. Pape, E. Perez, M. Peruzzi, A. Petrilli, G. Petrucciani, A. Pfeiffer, M. Pierini, F.M. Pitters, D. Rabady, A. Racz, T. Reis, G. Rolandi⁴⁴, M. Rovere, H. Sakulin, C. Schäfer, C. Schwick, M. Seidel, M. Selvaggi, A. Sharma, P. Silva, P. Sphicas⁴⁵, A. Stakia, J. Steggemann, M. Tosi, D. Treille, A. Tsirou, V. Veckalns⁴⁶, M. Verzetti, W.D. Zeuner

CERN, European Organization for Nuclear Research, Geneva, Switzerland

L. Caminada⁴⁷, K. Deiters, W. Erdmann, R. Horisberger, Q. Ingram, H.C. Kaestli, D. Kotlinski, U. Langenegger, T. Rohe, S.A. Wiederkehr

Paul Scherrer Institut, Villigen, Switzerland

M. Backhaus, L. Bäni, P. Berger, N. Chernyavskaya, G. Dissertori, M. Dittmar, M. Donegà, C. Dorfer, T.A. Gómez Espinosa, C. Grab, D. Hits, T. Klijnsma, W. Luster mann, R.A. Manzoni, M. Marionneau, M.T. Meinhard, F. Micheli, P. Musella, F. Nessi-Tedaldi, J. Pata, F. Pauss, G. Perrin, L. Perrozzi, S. Pigazzini, M. Quittnat, D. Ruini, D.A. Sanz Becerra, M. Schönenberger, L. Shchutska, V.R. Tavolaro, K. Theofilatos, M.L. Vesterbacka Olsson, R. Wallny, D.H. Zhu

ETH Zurich - Institute for Particle Physics and Astrophysics (IPA), Zurich, Switzerland

T.K. Aarrestad, C. Amsler⁴⁸, D. Brzhechko, M.F. Canelli, A. De Cosa, R. Del Burgo, S. Donato, C. Galloni, T. Hreus, B. Kilminster, S. Leontsinis, I. Neutelings, D. Pinna, G. Rauco, P. Robmann, D. Salerno, K. Schweiger, C. Seitz, Y. Takahashi, A. Zucchetta

Universität Zürich, Zurich, Switzerland

Y.H. Chang, K.y. Cheng, T.H. Doan, Sh. Jain, R. Khurana, C.M. Kuo, W. Lin, A. Pozdnyakov, S.S. Yu

National Central University, Chung-Li, Taiwan

P. Chang, Y. Chao, K.F. Chen, P.H. Chen, W.-S. Hou, Arun Kumar, Y.F. Liu, R.-S. Lu, E. Paganis, A. Psallidas, A. Steen

National Taiwan University (NTU), Taipei, Taiwan

B. Asavapibhop, N. Srimanobhas, N. Suwonjandee

Chulalongkorn University, Faculty of Science, Department of Physics, Bangkok, Thailand

M.N. Bakirci⁴⁹, A. Bat, F. Boran, S. Cerci⁵⁰, S. Damarseckin, Z.S. Demiroglu, F. Dolek, C. Dozen, I. Dumanoglu, E. Eskut, S. Girgis, G. Gokbulut, Y. Guler, E. Gurpinar, I. Hos⁵¹, C. Isik, E.E. Kangal⁵², O. Kara, U. Kiminsu, M. Oglakci, G. Onengut, K. Ozdemir⁵³, A. Polatoz, D. Sunar Cerci⁵⁰, U.G. Tok, S. Turkcapar, I.S. Zorbakir, C. Zorbilmez

Çukurova University, Physics Department, Science and Art Faculty, Adana, Turkey

B. Isildak⁵⁴, G. Karapinar⁵⁵, M. Yalvac, M. Zeyrek

Middle East Technical University, Physics Department, Ankara, Turkey

I.O. Atakisi, E. Gülmez, M. Kaya⁵⁶, O. Kaya⁵⁷, S. Ozkorucuklu⁵⁸, S. Tekten, E.A. Yetkin⁵⁹

Bogazici University, Istanbul, Turkey

M.N. Agaras, A. Cakir, K. Cankocak, Y. Komurcu, S. Sen⁶⁰

Istanbul Technical University, Istanbul, Turkey

B. Grynyov

Institute for Scintillation Materials of National Academy of Science of Ukraine, Kharkov, Ukraine

L. Levchuk

National Scientific Center, Kharkov Institute of Physics and Technology, Kharkov, Ukraine

F. Ball, L. Beck, J.J. Brooke, D. Burns, E. Clement, D. Cussans, O. Davignon, H. Flacher, J. Goldstein, G.P. Heath, H.F. Heath, L. Kreczko, D.M. Newbold⁶¹, S. Paramesvaran, B. Penning, T. Sakuma, D. Smith, V.J. Smith, J. Taylor, A. Titterton

University of Bristol, Bristol, United Kingdom

K.W. Bell, A. Belyaev⁶², C. Brew, R.M. Brown, D. Cieri, D.J.A. Cockerill, J.A. Coughlan, K. Harder, S. Harper, J. Linacre, E. Olaiya, D. Petyt, C.H. Shepherd-Themistocleous, A. Thea, I.R. Tomalin, T. Williams, W.J. Womersley

Rutherford Appleton Laboratory, Didcot, United Kingdom

R. Bainbridge, P. Bloch, J. Borg, S. Breeze, O. Buchmuller, A. Bundock, D. Colling, P. Dauncey, G. Davies, M. Della Negra, R. Di Maria, Y. Haddad, G. Hall, G. Iles, T. James, M. Komm, C. Laner, L. Lyons, A.-M. Magnan, S. Malik, A. Martelli, J. Nash⁶³, A. Nikitenko⁷, V. Palladino, M. Pesaresi, A. Richards, A. Rose, E. Scott, C. Seez, A. Shtipliyski, G. Singh, M. Stoye, T. Strebler, S. Summers, A. Tapper, K. Uchida, T. Virdee¹⁶, N. Wardle, D. Winterbottom, J. Wright, S.C. Zenz

Imperial College, London, United Kingdom

J.E. Cole, P.R. Hobson, A. Khan, P. Kyberd, C.K. Mackay, A. Morton, I.D. Reid, L. Teodorescu, S. Zahid

Brunel University, Uxbridge, United Kingdom

K. Call, J. Dittmann, K. Hatakeyama, H. Liu, C. Madrid, B. McMaster, N. Pastika, C. Smith

Baylor University, Waco, USA

R. Bartek, A. Dominguez

Catholic University of America, Washington DC, USA

A. Buccilli, S.I. Cooper, C. Henderson, P. Rumerio, C. West

The University of Alabama, Tuscaloosa, USA

D. Arcaro, T. Bose, D. Gastler, D. Rankin, C. Richardson, J. Rohlf, L. Sulak, D. Zou

Boston University, Boston, USA

G. Benelli, X. Coubez, D. Cutts, M. Hadley, J. Hakala, U. Heintz, J.M. Hogan⁶⁴, K.H.M. Kwok, E. Laird, G. Landsberg, J. Lee, Z. Mao, M. Narain, S. Sagir⁶⁵, R. Syarif, E. Usai, D. Yu

Brown University, Providence, USA

R. Band, C. Brainerd, R. Breedon, D. Burns, M. Calderon De La Barca Sanchez, M. Chertok, J. Conway, R. Conway, P.T. Cox, R. Erbacher, C. Flores, G. Funk, W. Ko, O. Kukral, R. Lander, M. Mulhearn, D. Pellett, J. Pilot, S. Shalhout, M. Shi, D. Stolp, D. Taylor, K. Tos, M. Tripathi, Z. Wang, F. Zhang

University of California, Davis, Davis, USA

M. Bachtis, C. Bravo, R. Cousins, A. Dasgupta, A. Florent, J. Hauser, M. Ignatenko, N. Mccoll, S. Regnard, D. Saltzberg, C. Schnaible, V. Valuev

University of California, Los Angeles, USA

E. Bouvier, K. Burt, R. Clare, J.W. Gary, S.M.A. Ghiasi Shirazi, G. Hanson, G. Karapostoli, E. Kennedy, F. Lacroix, O.R. Long, M. Olmedo Negrete, M.I. Paneva, W. Si, L. Wang, H. Wei, S. Wimpenny, B.R. Yates

University of California, Riverside, Riverside, USA

J.G. Branson, P. Chang, S. Cittolin, M. Derdzinski, R. Gerosa, D. Gilbert, B. Hashemi, A. Holzner, D. Klein, G. Kole, V. Krutelyov, J. Letts, M. Masciovecchio, D. Olivito, S. Padhi, M. Pieri, M. Sani, V. Sharma, S. Simon, M. Tadel, A. Vartak, S. Wasserbaech⁶⁶, J. Wood, F. Würthwein, A. Yagil, G. Zevi Della Porta

University of California, San Diego, La Jolla, USA

N. Amin, R. Bhandari, J. Bradmiller-Feld, C. Campagnari, M. Citron, A. Dishaw, V. Dutta, M. Franco Sevilla, L. Gouskos, R. Heller, J. Incandela, A. Ovcharova, H. Qu, J. Richman, D. Stuart, I. Suarez, S. Wang, J. Yoo

University of California, Santa Barbara - Department of Physics, Santa Barbara, USA

D. Anderson, A. Bornheim, J.M. Lawhorn, H.B. Newman, T.Q. Nguyen, M. Spiropulu, J.R. Vlimant, R. Wilkinson, S. Xie, Z. Zhang, R.Y. Zhu

California Institute of Technology, Pasadena, USA

M.B. Andrews, T. Ferguson, T. Mudholkar, M. Paulini, M. Sun, I. Vorobiev, M. Weinberg

Carnegie Mellon University, Pittsburgh, USA

J.P. Cumalat, W.T. Ford, F. Jensen, A. Johnson, M. Krohn, E. MacDonald, T. Mulholland, R. Patel, K. Stenson, K.A. Ulmer, S.R. Wagner

University of Colorado Boulder, Boulder, USA

J. Alexander, J. Chaves, Y. Cheng, J. Chu, A. Datta, K. Mcdermott, N. Mirman, J.R. Patterson, D. Quach, A. Rinkevicius, A. Ryd, L. Skinnari, L. Soffi, S.M. Tan, Z. Tao, J. Thom, J. Tucker, P. Wittich, M. Zientek

Cornell University, Ithaca, USA

S. Abdullin, M. Albrow, M. Alyari, G. Apollinari, A. Apresyan, A. Apyan, S. Banerjee, L.A.T. Bauerdick, A. Beretvas, J. Berryhill, P.C. Bhat, G. Bolla[†], K. Burkett, J.N. Butler, A. Canepa, G.B. Cerati, H.W.K. Cheung, F. Chlebana, M. Cremonesi, J. Duarte, V.D. Elvira, J. Freeman, Z. Gecse, E. Gottschalk, L. Gray, D. Green, S. Grünendahl, O. Gutsche, J. Hanlon, R.M. Harris, S. Hasegawa, J. Hirschauer, Z. Hu, B. Jayatilaka, S. Jindariani, M. Johnson, U. Joshi, B. Klima, M.J. Kortelainen, B. Kreis, S. Lammel, D. Lincoln, R. Lipton, M. Liu, T. Liu, J. Lykken, K. Maeshima, J.M. Marraffino, D. Mason, P. McBride, P. Merkel, S. Mrenna, S. Nahn, V. O'Dell, K. Pedro, C. Pena, O. Prokofyev, G. Rakness, L. Ristori, A. Savoy-Navarro⁶⁷,

B. Schneider, E. Sexton-Kennedy, A. Soha, W.J. Spalding, L. Spiegel, S. Stoynev, J. Strait, N. Strobbe, L. Taylor, S. Tkaczyk, N.V. Tran, L. Uplegger, E.W. Vaandering, C. Vernieri, M. Verzocchi, R. Vidal, M. Wang, H.A. Weber, A. Whitbeck

Fermi National Accelerator Laboratory, Batavia, USA

D. Acosta, P. Avery, P. Bortignon, D. Bourilkov, A. Brinkerhoff, L. Cadamuro, A. Carnes, M. Carver, D. Curry, R.D. Field, S.V. Gleyzer, B.M. Joshi, J. Konigsberg, A. Korytov, K.H. Lo, P. Ma, K. Matchev, H. Mei, G. Mitselmakher, D. Rosenzweig, K. Shi, D. Sperka, J. Wang, S. Wang, X. Zuo

University of Florida, Gainesville, USA

Y.R. Joshi, S. Linn

Florida International University, Miami, USA

A. Ackert, T. Adams, A. Askew, S. Hagopian, V. Hagopian, K.F. Johnson, T. Kolberg, G. Martinez, T. Perry, H. Prosper, A. Saha, C. Schiber, R. Yohay

Florida State University, Tallahassee, USA

M.M. Baarmand, V. Bhopatkar, S. Colafranceschi, M. Hohlmann, D. Noonan, M. Rahmani, T. Roy, F. Yumiceva

Florida Institute of Technology, Melbourne, USA

M.R. Adams, L. Apanasevich, D. Berry, R.R. Betts, R. Cavanaugh, X. Chen, S. Dittmer, O. Evdokimov, C.E. Gerber, D.A. Hangal, D.J. Hofman, K. Jung, J. Kamin, C. Mills, I.D. Sandoval Gonzalez, M.B. Tonjes, H. Trauger, N. Varelas, H. Wang, X. Wang, Z. Wu, J. Zhang

University of Illinois at Chicago (UIC), Chicago, USA

M. Alhusseini, B. Bilki ⁶⁸, W. Clarida, K. Dilsiz ⁶⁹, S. Durgut, R.P. Gandrajula, M. Haytmyradov, V. Khristenko, J.-P. Merlo, A. Mestvirishvili, A. Moeller, J. Nachtman, H. Ogul ⁷⁰, Y. Onel, F. Ozok ⁷¹, A. Penzo, C. Snyder, E. Tiras, J. Wetzel

The University of Iowa, Iowa City, USA

B. Blumenfeld, A. Cocoros, N. Eminizer, D. Fehling, L. Feng, A.V. Gritsan, W.T. Hung, P. Maksimovic, J. Roskes, U. Sarica, M. Swartz, M. Xiao, C. You

Johns Hopkins University, Baltimore, USA

A. Al-bataineh, P. Baringer, A. Bean, S. Boren, J. Bowen, A. Bylinkin, J. Castle, S. Khalil, A. Kropivnitskaya, D. Majumder, W. Mcbrayer, M. Murray, C. Rogan, S. Sanders, E. Schmitz, J.D. Tapia Takaki, Q. Wang

The University of Kansas, Lawrence, USA

S. Duric, A. Ivanov, K. Kaadze, D. Kim, Y. Maravin, D.R. Mendis, T. Mitchell, A. Modak, A. Mohammadi, L.K. Saini, N. Skhirtladze

Kansas State University, Manhattan, USA

F. Rebassoo, D. Wright

Lawrence Livermore National Laboratory, Livermore, USA

A. Baden, O. Baron, A. Belloni, S.C. Eno, Y. Feng, C. Ferraioli, N.J. Hadley, S. Jabeen, G.Y. Jeng, R.G. Kellogg, J. Kunkle, A.C. Mignerey, S. Nabili, F. Ricci-Tam, Y.H. Shin, A. Skuja, S.C. Tonwar, K. Wong

University of Maryland, College Park, USA

D. Abercrombie, B. Allen, V. Azzolini, A. Baty, G. Bauer, R. Bi, S. Brandt, W. Busza, I.A. Cali, M. D'Alfonso, Z. Demiragli, G. Gomez Ceballos, M. Goncharov, P. Harris, D. Hsu, M. Hu, Y. Iiyama, G.M. Innocenti, M. Klute, D. Kovalskyi, Y.-J. Lee, P.D. Luckey, B. Maier, A.C. Marini, C. Mcginn, C. Mironov, S. Narayanan, X. Niu, C. Paus, C. Roland, G. Roland, G.S.F. Stephans, K. Sumorok, K. Tatar, D. Velicanu, J. Wang, T.W. Wang, B. Wyslouch, S. Zhaozhong

Massachusetts Institute of Technology, Cambridge, USA

A.C. Benvenuti, R.M. Chatterjee, A. Evans, P. Hansen, S. Kalafut, Y. Kubota, Z. Lesko, J. Mans, N. Ruckstuhl, R. Rusack, J. Turkewitz, M.A. Wadud

University of Minnesota, Minneapolis, USA

J.G. Acosta, S. Oliveros

University of Mississippi, Oxford, USA

E. Avdeeva, K. Bloom, D.R. Claes, C. Fangmeier, F. Golf, R. Gonzalez Suarez, R. Kamalieddin, I. Kravchenko, J. Monroy, J.E. Siado, G.R. Snow, B. Stieger

University of Nebraska-Lincoln, Lincoln, USA

A. Godshalk, C. Harrington, I. Iashvili, A. Kharchilava, C. Mclean, D. Nguyen, A. Parker, S. Rappoccio, B. Roozbahani

State University of New York at Buffalo, Buffalo, USA

G. Alverson, E. Barberis, C. Freer, A. Hortiangtham, D.M. Morse, T. Orimoto, R. Teixeira De Lima, T. Wamorkar, B. Wang, A. Wisecarver, D. Wood

Northeastern University, Boston, USA

S. Bhattacharya, O. Charaf, K.A. Hahn, N. Mucia, N. Odell, M.H. Schmitt, K. Sung, M. Trovato, M. Velasco

Northwestern University, Evanston, USA

R. Bucci, N. Dev, M. Hildreth, K. Hurtado Anampa, C. Jessop, D.J. Karmgard, N. Kellams, K. Lannon, W. Li, N. Loukas, N. Marinelli, F. Meng, C. Mueller, Y. Musienko³⁵, M. Planer, A. Reinsvold, R. Ruchti, P. Siddireddy, G. Smith, S. Taroni, M. Wayne, A. Wightman, M. Wolf, A. Woodard

University of Notre Dame, Notre Dame, USA

J. Alimena, L. Antonelli, B. Bylsma, L.S. Durkin, S. Flowers, B. Francis, A. Hart, C. Hill, W. Ji, T.Y. Ling, W. Luo, B.L. Winer

The Ohio State University, Columbus, USA

S. Cooperstein, P. Elmer, J. Hardenbrook, S. Higginbotham, A. Kalogeropoulos, D. Lange, M.T. Lucchini, J. Luo, D. Marlow, K. Mei, I. Ojalvo, J. Olsen, C. Palmer, P. Piroué, J. Salfeld-Nebgen, D. Stickland, C. Tully

Princeton University, Princeton, USA

S. Malik, S. Norberg

University of Puerto Rico, Mayaguez, USA

A. Barker, V.E. Barnes, S. Das, L. Gutay, M. Jones, A.W. Jung, A. Khatiwada, B. Mahakud, D.H. Miller, N. Neumeister, C.C. Peng, S. Piperov, H. Qiu, J.F. Schulte, J. Sun, F. Wang, R. Xiao, W. Xie

Purdue University, West Lafayette, USA

T. Cheng, J. Dolen, N. Parashar

Purdue University Northwest, Hammond, USA

Z. Chen, K.M. Ecklund, S. Freed, F.J.M. Geurts, M. Kilpatrick, W. Li, B.P. Padley, J. Roberts, J. Rorie, W. Shi, Z. Tu, J. Zabel, A. Zhang

Rice University, Houston, USA

A. Bodek, P. de Barbaro, R. Demina, Y.t. Duh, J.L. Dulemba, C. Fallon, T. Ferbel, M. Galanti, A. Garcia-Bellido, J. Han, O. Hindrichs, A. Khukhunaishvili, P. Tan, R. Taus

University of Rochester, Rochester, USA

R. Ciesielski

The Rockefeller University, New York, USA

A. Agapitos, J.P. Chou, Y. Gershtein, E. Halkiadakis, M. Heindl, E. Hughes, S. Kaplan, R. Kunnawalkam Elayavalli, S. Kyriacou, A. Lath, R. Montalvo, K. Nash, M. Osherson, H. Saka, S. Salur, S. Schnetzer, D. Sheffield, S. Somalwar, R. Stone, S. Thomas, P. Thomassen, M. Walker

Rutgers, The State University of New Jersey, Piscataway, USA

A.G. Delannoy, J. Heideman, G. Riley, S. Spanier

University of Tennessee, Knoxville, USA

O. Bouhali⁷², A. Celik, M. Dalchenko, M. De Mattia, A. Delgado, S. Dildick, R. Eusebi, J. Gilmore, T. Huang, T. Kamon⁷³, S. Luo, R. Mueller, A. Perloff, L. Perniè, D. Rathjens, A. Safonov

Texas A&M University, College Station, USA

N. Akchurin, J. Damgov, F. De Guio, P.R. Duderø, S. Kunori, K. Lamichhane, S.W. Lee, T. Mengke, S. Muthumuni, T. Peltola, S. Undleeb, I. Volobouev, Z. Wang

Texas Tech University, Lubbock, USA

S. Greene, A. Gurrola, R. Janjam, W. Johns, C. Maguire, A. Melo, H. Ni, K. Padeken, J.D. Ruiz Alvarez, P. Sheldon, S. Tuo, J. Velkovska, M. Verweij, Q. Xu

Vanderbilt University, Nashville, USA

M.W. Arenton, P. Barria, B. Cox, R. Hirosky, M. Joyce, A. Ledovskoy, H. Li, C. Neu, T. Sinthuprasith, Y. Wang, E. Wolfe, F. Xia

University of Virginia, Charlottesville, USA

R. Harr, P.E. Karchin, N. Poudyal, J. Sturdy, P. Thapa, S. Zaleski

Wayne State University, Detroit, USA

M. Brodski, J. Buchanan, C. Caillol, D. Carlsmith, S. Dasu, L. Dodd, B. Gomber, M. Grothe, M. Herndon, A. Hervé, U. Hussain, P. Klabbers, A. Lanaro, K. Long, R. Loveless, T. Ruggles, A. Savin, V. Sharma, N. Smith, W.H. Smith, N. Woods

University of Wisconsin - Madison, Madison, WI, USA

[†] Deceased.

¹ Also at Vienna University of Technology, Vienna, Austria.

² Also at IRFU, CEA, Université Paris-Saclay, Gif-sur-Yvette, France.

³ Also at Universidade Estadual de Campinas, Campinas, Brazil.

⁴ Also at Federal University of Rio Grande do Sul, Porto Alegre, Brazil.

⁵ Also at Université Libre de Bruxelles, Bruxelles, Belgium.

⁶ Also at University of Chinese Academy of Sciences, Beijing, China.

⁷ Also at Institute for Theoretical and Experimental Physics, Moscow, Russia.

⁸ Also at Joint Institute for Nuclear Research, Dubna, Russia.

⁹ Now at Cairo University, Cairo, Egypt.

¹⁰ Also at Fayoum University, El-Fayoum, Egypt.

- 11 Now at British University in Egypt, Cairo, Egypt.
- 12 Also at Department of Physics, King Abdulaziz University, Jeddah, Saudi Arabia.
- 13 Also at Université de Haute Alsace, Mulhouse, France.
- 14 Also at Skobeltsyn Institute of Nuclear Physics, Lomonosov Moscow State University, Moscow, Russia.
- 15 Also at Tbilisi State University, Tbilisi, Georgia.
- 16 Also at CERN, European Organization for Nuclear Research, Geneva, Switzerland.
- 17 Also at RWTH Aachen University, III. Physikalisches Institut A, Aachen, Germany.
- 18 Also at University of Hamburg, Hamburg, Germany.
- 19 Also at Brandenburg University of Technology, Cottbus, Germany.
- 20 Also at MTA-ELTE Lendület CMS Particle and Nuclear Physics Group, Eötvös Loránd University, Budapest, Hungary.
- 21 Also at Institute of Nuclear Research ATOMKI, Debrecen, Hungary.
- 22 Also at Institute of Physics, University of Debrecen, Debrecen, Hungary.
- 23 Also at Indian Institute of Technology Bhubaneswar, Bhubaneswar, India.
- 24 Also at Institute of Physics, Bhubaneswar, India.
- 25 Also at Shoolini University, Solan, India.
- 26 Also at University of Visva-Bharati, Santiniketan, India.
- 27 Also at Isfahan University of Technology, Isfahan, Iran.
- 28 Also at Plasma Physics Research Center, Science and Research Branch, Islamic Azad University, Tehran, Iran.
- 29 Also at Università degli Studi di Siena, Siena, Italy.
- 30 Also at Kyunghee University, Seoul, Republic of Korea.
- 31 Also at International Islamic University of Malaysia, Kuala Lumpur, Malaysia.
- 32 Also at Malaysian Nuclear Agency, MOSTI, Kajang, Malaysia.
- 33 Also at Consejo Nacional de Ciencia y Tecnología, Mexico city, Mexico.
- 34 Also at Warsaw University of Technology, Institute of Electronic Systems, Warsaw, Poland.
- 35 Also at Institute for Nuclear Research, Moscow, Russia.
- 36 Now at National Research Nuclear University 'Moscow Engineering Physics Institute' (MEPhI), Moscow, Russia.
- 37 Also at St. Petersburg State Polytechnical University, St. Petersburg, Russia.
- 38 Also at University of Florida, Gainesville, USA.
- 39 Also at P.N. Lebedev Physical Institute, Moscow, Russia.
- 40 Also at Budker Institute of Nuclear Physics, Novosibirsk, Russia.
- 41 Also at Faculty of Physics, University of Belgrade, Belgrade, Serbia.
- 42 Also at INFN Sezione di Pavia ^a, Università di Pavia ^b, Pavia, Italy.
- 43 Also at University of Belgrade, Faculty of Physics and Vinca Institute of Nuclear Sciences, Belgrade, Serbia.
- 44 Also at Scuola Normale e Sezione dell'INFN, Pisa, Italy.
- 45 Also at National and Kapodistrian University of Athens, Athens, Greece.
- 46 Also at Riga Technical University, Riga, Latvia.
- 47 Also at Universität Zürich, Zurich, Switzerland.
- 48 Also at Stefan Meyer Institute for Subatomic Physics (SMI), Vienna, Austria.
- 49 Also at Gaziosmanpasa University, Tokat, Turkey.
- 50 Also at Adiyaman University, Adiyaman, Turkey.
- 51 Also at Istanbul Aydin University, Istanbul, Turkey.
- 52 Also at Mersin University, Mersin, Turkey.
- 53 Also at Piri Reis University, Istanbul, Turkey.
- 54 Also at Ozyegin University, Istanbul, Turkey.
- 55 Also at Izmir Institute of Technology, Izmir, Turkey.
- 56 Also at Marmara University, Istanbul, Turkey.
- 57 Also at Kafkas University, Kars, Turkey.
- 58 Also at Istanbul University, Faculty of Science, Istanbul, Turkey.
- 59 Also at Istanbul Bilgi University, Istanbul, Turkey.
- 60 Also at Hacettepe University, Ankara, Turkey.
- 61 Also at Rutherford Appleton Laboratory, Didcot, United Kingdom.
- 62 Also at School of Physics and Astronomy, University of Southampton, Southampton, United Kingdom.
- 63 Also at Monash University, Faculty of Science, Clayton, Australia.
- 64 Also at Bethel University, St. Paul, USA.
- 65 Also at Karamanoğlu Mehmetbey University, Karaman, Turkey.
- 66 Also at Utah Valley University, Orem, USA.
- 67 Also at Purdue University, West Lafayette, USA.
- 68 Also at Beykent University, Istanbul, Turkey.
- 69 Also at Bingol University, Bingol, Turkey.
- 70 Also at Sinop University, Sinop, Turkey.
- 71 Also at Mimar Sinan University, Istanbul, Istanbul, Turkey.
- 72 Also at Texas A&M University at Qatar, Doha, Qatar.
- 73 Also at Kyungpook National University, Daegu, Republic of Korea.